ARGEMIRO TEIXEIRA LEITE FILHO

IMPACTS OF DEFORESTATION ON THE SOUTHERN AMAZON RAINY SEASON

Dissertation submitted to the Applied Meteorology Graduate Program of the Universidade Federal de Viçosa in partial fulfillment of the requirements for the degree of *Magister Scientiae*.

VIÇOSA
MINAS GERAIS – BRASIL
2019

Ficha catalográfica preparada pela Biblioteca Central da Universidade Federal de Viçosa - Câmpus Viçosa

T
L533i
2019

Leite Filho, Argemiro Teixeira, 1991-
Impacts of deforestation on the Southern Amazon rainy season / Argemiro Teixeira Leite Filho. – Viçosa, MG, 2019.
xix, 77 f. : il. (algumas color.) ; 29 cm.

Texto em inglês.
Inclui apêndice.
Orientador: Marcos Heil Costa.
Dissertação (mestrado) - Universidade Federal de Viçosa.
Referências bibliográficas: f. 58-69.

1. Meteorologia agrícola - Amazônia. 2. Amazônia. 3. Desmatamento. 4. Secas - Amazônia. 5. Chuvas - Amazônia. I. Universidade Federal de Viçosa. Departamento de Engenharia Agrícola. Programa de Pós-Graduação em Meteorologia Agrícola. II. Título.

CDD 22. ed. 630.2515

ARGEMIRO TEIXEIRA LEITE FILHO

IMPACTS OF DEFORESTATION ON THE SOUTHERN AMAZON RAINY SEASON

Dissertation submitted to the Applied Meteorology Graduate Program of the Universidade Federal de Viçosa in partial fulfillment of the requirements for the degree of *Magister Scientiae*.

APPROVED: February 18, 2019.

Gilvan Sampaio de Oliveira

Gabrielle Ferreira Pires

Marcos Heil Costa
(Adviser)

This dissertation is dedicated to my parents, Valmisa and Argemiro.

“I are irrevocably on a path that will lead us to the stars. Unless, by a monstrous capitulation to selfishness and stupidity, I end up destroying ourselves.”

Carl Sagan

ACKNOWLEDGMENTS

To God (or any other name that calls it), the supreme energy and intelligence of the universe and the primary cause of everything, by wisdom and protection.

To my spiritual protectors, I thank for everything that is placed in my path. What does not bring me happiness allows me to recognize it when it arrives.

To my Father Argemiro, who I has the immense pride of bearing his name, for teaching me that honesty and humility lead anyone to their objectives, always encouraging me. To my mother Valmisa, for being strength and encouragement that keeps me standing with her genuine love. My friend and angel. Through her example as an educator I was able to appreciate the value of the study. My eternal literacy teacher.

To my sister Joyce, for providing me with fraternal love, understanding, trust, and friendship in its purest form.

To my nephews: Maria Eduarda, João Mateus, Levy and Sophya. Your smile and your innocence make me have the strength to follow. With you my life has gained another meaning. Thank you for all the color you put in my world.

To my four-legged companion, Dora, who, anxiously, always expected me to come from the university with the most sincere love to offer.

To the two special people who disincarnated during this walk, but who are present in another plan: My grandfather Osvaldo and my aunt friend Regina.

To professor and great scientist Marcos Heil Costa, for the opportunity he gave me three and a half years ago, when he trusted me to be part of his team, opening the doors of the scientific career. I am grateful for the challenges provided, for it is through them that I have been striving to be better. My gratitude also for all the teachings and opportunities. It is impossible to measure how much it evolves under its guidance.

To colleagues, friends and members of the Research Group on Atmosphere-Biosphere Interaction and Applied Meteorology Program, for companionship at all times, whether in meetings with beer and guitar, or in the most intense moments of our academic routine. Aninha, Carol, Emily, Fabi, Gabi, Lucas, Matheus, Marina, Pauline, Raphael, Vinícius, Vitor Benezoli, Vitor Fontes and Luís, thank you for the pleasant coexistence, for all help, encouragement and attention. Aside from co-workers, I have made great friends that I will bring to life.

I am especially grateful to Lívia Dias for the careful reading and precious comments in the first chapter of this dissertation and for attention in my first steps within the group. To Gabriel Abrahão, for the indispensable help in the automation of the analyzes, discussions, fundamental tips and incentive. To Fernando Pimenta,

for the competent help in geoprocessing, attending to my most perfectionists requests and to Verônica Pontes, who contributed much to this work during his intership.

I thank the Federal University of Viçosa, a young lady of more than 90 years, for providing me with more than I expected. In particular to Department of Agricultural Engineering for the opportunity to complete this stage.

To all Teachers of Applied Meteorology Graduate Program of the Federal University of Viçosa, by the knowledge transmitted and to Graça, competent secretary, for help and attention without measuring efforts.

To the National Council for Scientific and Technological Development (CNPq), for granting the scholarship and the Association of Farmers and Irrigators of Bahia (AIBA), for granting the research grant in recent months.

To all who contributed to the conclusion of this stage, even if I did not mention it, especially to those who accompanied me on cloudy days. I do not linger here, for words are unnecessary to those who are grateful.

SUMMARY

LIST OF FIGURES

CHAPTER 1

CHAPTER 2

LIST OF TABLES

CHAPTER 1

LIST OF ACRONYMS

ANA	*Agência Nacional de Águas* (National Water Agency)
BHALU	Brazilian Historical Agricultural Land Use database
CAR	*Cadastro Ambiental Rural* (Rural Environmental Registry)
CDF	Cumulative Probability Density Function
FAO	Food and Agriculture Organization
HidroWeb	*Sistema de Informações Hidrológicas* (Hydrological Information System)
IBGE	*Instituto Brasileiro de Geografia e Estatística* (Brazilian Institute of geography and statistics)
INPE	*Instituto Nacional de Pesquisas Espaciais* (National Institute for Space Research)
IPEA	Institute for Applied Economic Research
ITCZ	Inter-Tropical Convergence Zone
LAI	Leaf Area Index
MAE	Mean absolute error
NASA	National Aeronautics and Space Administration
NCAR	National Center for Atmospheric Research
NCEP	National Centers for Environmental Prediction
NOAA	National Oceanic and Atmospheric Administration
OECD	Organization for Economic Co-operation and Development
RG	Rain Gauge
RMSE	Root-mean square error
SACZ	South Atlantic Convergence Zone
SCMP	Mechanism of the shallow convection moisture pump

SST	Sea Surface Temperature
TRMM	Tropical Rainfall Measuring Mission

LIST OF SYMBOLS

$\overline{B}'_{i,j,t}$	Mean of onset anomalies
$\widehat{B}_{i,j}$	Estimated onset of the rainy season due to geographical position
$\overline{B_t}$	Annual averages of onset of the rainy season
$\overline{E}'_{i,j,t}$	Mean of demise anomalies
$\widehat{E}_{i,j}$	Estimated demise of the rainy season due to geographical position
$\overline{E_t}$	Annual averages of demise of the rainy season
$\overline{L}'_{i,j,t}$	Mean of length anomalies
$\widehat{L}_{i,j}$	Estimated length of the rainy season due to geographical position
$\overline{L_t}$	Annual averages of length of the rainy season
$B_{i,j,t}$	Onset of the rainy season
$B'_{i,j,t}$	Anomalies of rainy season onset
$E_{i,j,t}$	Demise of the rainy season
$E'_{i,j,t}$	Anomalies of rainy season demise
$L_{i,j,t}$	Length of the rainy season
$L'_{i,j,t}$	Anomalies of rainy season length
$N4'_t$	Tropical sea surface temperature anomalies of region Niño4
AA	Anomalous Accumulation of rainfall
$D_{i,j,t}$	Percentage of a pixel that is deforested
$DS_{i,j,t}$	Dry Spell events
MA	Late rainy season (March and April)
NDJF	Peak rainy season (November, December, January and February)
SO	Early rainy season (September and October, post-onset)
t	Year

λ	Longitude
φ	Latitude
φ_{SJ}	Southern Hemisphere subtropical jet position

ABSTRACT

LEITE FILHO, Argemiro Teixeira, M.Sc., Universidade Federal de Viçosa, February, 2019. **Impacts of deforestation on the southern Amazon rainy season.** Adviser: Marcos Heil Costa.

Amazonian deforestation is causing notable changes in the hydrological cycle by altering important precipitation characteristics. Past studies presented evidence that deforestation may affect the precipitation seasonality in southern Amazonia. This work provides an integrated research on how decades of deforestation in southern Amazonia have affected the regional rainy season. In Chapter 1, I used daily rainfall time series data from 112 rain gauges and a recent yearly 1-km land use dataset covering the period from 1974 to 2012 to evaluate the effects of the extent of deforestation at different spatial scales on the onset of the rainy season and on the duration of dry spells in southern Amazonia. In Chapter 2, I used daily rainfall data from TRMM 3B42 product and a recent yearly 1-km land use dataset to evaluate the quantitative effects of deforestation on the onset, demise and length of the rainy season in southern Amazonia for a period of 15 years (1998-2012). Additionally, I used Niño4 anomalies, zonal wind data and deforestation data to explain and predict the interannual variability of the rainy season onset. Using rain gauge data, correlation analyses indicate a delay in the onset of 1.2–1.7 days per each 10% increase in deforestation. Analysis of cumulative probability density functions emphasized that the likelihood of rainy season onset occurring earlier than normal decreases as the local deforestation fraction increases. In addition, the probability of occurrence of dry spells in the early and late rainy season is higher in areas with greater deforestation. Using precipitation remote sensing products, onset has delayed ~0.38±0.05 days per year (5.7±0.75 days in 15 years), demise has advanced 1.34±0.76 days per year (20±11.4 days in 15 years) and the rainy season has shortened by 1.81±0.97 days per year (27±14.5 days in 15 years). Onset, demise and length also present meridional and zonal gradients linked to large-scale climate mechanisms. After removing the effects related to geographical position and year, I also verified a relationship between onset, demise and length and deforestation: Onset delays ~0.4±0.12 day, demise advances ~1.0±0.22 day and length decreases ~0.9±0.34 day per each 10% increase in deforestation. I also presented empirical evidence of the interaction between large-scale and local-scale processes, with

interannual variation of the onset in the region explained by Niño4 sea surface temperature anomalies, Southern Hemisphere subtropical jet position, deforestation and their interactions ($r^2 = 69\%$, $p < 0.001$, MAE = 2.7 days). The delayed onset, advanced demise, shorter length of the rainy season and longer dry spell events in highly deforested areas increase the climate risk to agriculture in the region.

RESUMO

LEITE FILHO, Argemiro Teixeira, M.Sc., Universidade Federal de Viçosa, fevereiro de 2019. **Impactos do desmatamento na estação chuvosa do sul da Amazônia.** Orientador: Marcos Heil Costa.

O desmatamento da Amazônia vem causando mudanças notáveis no ciclo hidrológico, alterando importantes características da precipitação. Estudos anteriores apresentaram evidências de que o desmatamento pode afetar a sazonalidade da precipitação no sul da Amazônia. Este trabalho fornece uma pesquisa integrada sobre como décadas de desmatamento no sul da Amazônia afetaram a estação chuvosa. No Capítulo 1, utilizei dados diários de precipitação de 112 séries temporais advindas de pluviômetros e um recente banco de dados anuais de uso do solo com resolução de 1 km x 1 km englobando o período de 1974 a 2012 para avaliar os efeitos da extensão do desmatamento em diferentes escalas espaciais no início da estação chuvosa e na duração dos veranicos. No Capítulo 2, utilizei dados diários de precipitação TRMM produto 3B42 e o mesmo conjunto de dados anuais de uso do solo para avaliar os efeitos quantitativos do desmatamento no início, fim e duração da estação chuvosa por um período de 15 anos (1998-2012). Além disso, utilizei anomalias do Niño4, dados de vento zonal e dados de desmatamento para explicar e prever a variabilidade interanual do início da estação chuvosa. Utilizando dados advindos de pluviômetros, as análises de correlação indicam um atraso no início da estação chuvosa de ~1,2 a 1,7 dias por cada aumento de 10% no desmatamento. A análise das funções de densidade cumulativa de probabilidade enfatizaram que a probabilidade do início da estação chuvosa ocorrer antes do normal diminui à medida que a fração de desmatamento local aumenta. Além disso, a probabilidade de ocorrência de veranicos no início e no fim da estação chuvosa é maior em áreas com maior desmatamento. Utilizando produtos de precipitação por sensoriamento remoto, o início da estação chuvosa atrasou ~0,38±0,05 dias por ano (5,7±0,75 dias em 15 anos), o fim adiantou ~1,34 ±0,76 dias por ano (20±11,4 dias em 15 anos) e a estação chuvosa se mostrou ~1,81 ± 0,97 dias menor a cada ano (27±14,5 dias em 15 anos). O início, o fim e a duração da estação chuvosa também apresentaram gradientes meridional e zonal ligados a mecanismos climáticos de grande escala. Após remover os efeitos relacionados à posição geográfica e ao ano, também verifiquei uma relação entre o início, fim e duração da estação chuvosa com o desmatamento: atraso no

início de ~0,4±0,12 dia, adianto no fim de ~1,0±0,22 dia e decréscimo no comprimento da estação chuvosa de ~0,9±0,34 dia a cada aumento de 10% no desmatamento. Utilizando anomalias de temperatura do Niño4, a posição do jato subtropical do Hemisfério Sul, dados de desmatamento e suas interações, apresentei evidências empíricas da interação entre processos de grande escala e de escala local afetando o início da estação chuvosa na região (r^2 = 69%, p <0,001, MAE = 2,7 dias). O atraso no início, o fim precoce, a duração da estação chuvosa mais curta e a maior ocorrência de veranicos em áreas mais desmatadas aumentam o risco climático para a agricultura na região.

GENERAL INTRODUCTION

The Amazon forest acts as an indispensable source of heat for the atmosphere through its intense evapotranspiration and latent heat release (Marengo, 2006; Malhi et al., 2008; Satyamurty et al., 2013). Despite its importance, the Amazon is facing a multitude of threats as a result of unsustainable economic development (Fearnside, 2005). By 2017, 20% of land forested before 1970 had been deforested (INPE, 2018).

Although cattle ranching remains the dominant use of cleared land, the growing importance of larger and faster conversion to cropland (principally soybean) has defined a trend of forest loss in Amazonia since the early 2000s (Morton et al., 2006). In the southern Amazon only, changes in land cover from 1970 to 2012 affected 191,319 km² (Dias et al., 2016).

Deforestation threaten the maintenance of critical ecosystem services important for the whole world, and especially for Brazil itself, including the recycling water that provides rainfall to Amazonia (Fearnside, 2008). Field observations and

numerical studies reveal that deforestation in Amazonia could alter the regional hydroclimate (Costa and Pires, 2010; Butt et al., 2011; Debortoli et al., 2015; Debortoli et al., 2016; Wright et al., 2017), influencing the amount of sensible heating over the land, creating instability and upward motion (Khanna et al., 2017). However, the quantitative role of deforestation in altering the precipitation seasonality remains partially unclear.

The knowledge of the precipitation's patterns and how it is affected by changes in the land cover is critical to the management of water resources and consequently to the management of agricultural production. Thus, these changes that are of concern to southern Amazon. The rainy season is a large-scale limiting factor for double-cropping systems, largely practiced in the region (Spangler et al., 2017, Abrahão and Costa, 2018).

In this context, this work provides an integrated research on how decades of deforestation in southern Amazonia have affected the regional rainy season and provides quantitative estimates so that the effects of deforestation can be predicted with a focus on impacts to agriculture. I investigate the possible role of reduced vegetation cover in contributing to a more frequent occurrence of longer dry spells, delayed onset, advanced demise and lower length of the rainy season in southern Amazon. Additionally, I investigate an interaction between the local-scale processes and the large-scale mechanisms to determine and predict the interannual variation of the onset over the region.

To achieve these goals, this dissertation is structured in three chapters. In the Chapter 1, I investigated the effects of deforestation on the rainy season onset and the duration of dry spells in southern Amazonia using rain gauge data and a recent yearly 1-km land use database. In the chapter 2, I evaluated the impacts of deforestation on

the onset, demise and length of the southern Amazon rainy season using remote sensing precipitation product and the same land-use database used previously. Finally, in the Chapter 3, dissertation overview, general implications, recommendations and future challenges are presented.

CHAPTER 1 - EFFECTS OF DEFORESTATION ON THE ONSET OF THE RAINY SEASON AND THE DURATION OF DRY SPELLS IN SOUTHERN AMAZONIA

LEITE-FILHO, A. T., SOUSA PONTES, V. Y., AND COSTA, M. H. **Effects of deforestation on the onset of the rainy season and the duration of dry spells in southern Amazonia.** Journal of Geophysical Research: Atmospheres, 2019. 124. https://doi.org/10.1029/2018JD029537

1.1. Introduction

The Brazilian economic model of land use and exploitation of natural resources, characterized by the expansion of agricultural lands, predatory exploitation of timber, and accelerated urbanization, has caused great devastation to the Amazon biome, beginning around the end of the 1970s and continuing to the present.

Deforestation modifies some land surface properties that can affect both the amount and the partitioning of available energy on the surface. Forest removal increases the surface albedo and reduces the available net surface radiation. Furthermore, deforestation changes the partitioning of net radiation into latent and

sensible heat flux by reducing surface roughness, leaf area index (LAI), and root depth. When compared to forested sites, deforested areas have higher albedo (18% compared to 13%; Culf et al., 1996), lower soil moisture storage capacity (because grasses have shallow root systems), and drier soils, all of which contribute to decreasing the latent heat flux. Cleared land may have a latent heat flux 30% lower than that of forested land (Gash and Nobre, 1997), and this means that stronger moisture transport and deeper convection are needed to trigger rainfall. In addition, reduced surface roughness decreases atmospheric turbulence and weakens vertical motion (Khanna and Medvigy, 2014).

In a region where precipitation is mainly convective (Marengo, 1995), these changes in land–atmosphere interaction may have caused important modifications in the regional hydroclimate, interfering in the hydrological cycle and altering important precipitation characteristics. Using 16 historical time series of precipitation for the state of Rondônia collected between 1961 and 2008, Butt et al. (2011) demonstrated that current trends in the delay in rainy season onset may be as great as 0.6 days per year, and after 30 years of deforestation, the onset was estimated to be 18 days later on average than it was before deforestation. Debortoli et al. (2015) also found delayed onset of the southern Amazon rainy season in more than 88% of the 200 rain gauges analyzed in the 1971–2010 period.

In addition to pointing out changes in precipitation timing, recent studies indicate that different hydroclimatic changes may be caused by different spatial scales of deforestation. Studying the onset of the rainy season, Debortoli et al. (2016) showed that rainfall seasonality is not correlated with forest cover at the microscale (1–15 km) but significant correlations appear at the mesoscale (30–50 km). This suggests that mesoscale atmospheric processes influenced by the land surface may have a greater influence on the onset of the rainy season.

More recently, Khanna et al. (2017) explored controls on dry-to-wet season precipitation in Rondônia in southern Amazonia, concluding that changes in land cover affect the atmospheric circulation at the mesoscale, with rainfall typically decreasing over deforested areas. Chambers and Artaxo (2017), commenting on the results obtained by Khanna et al. (2017), raised the hypothesis that this shift in surface roughness would modify forest–atmosphere interactions, suggesting that deforestation is sufficiently advanced to have caused a shift from a thermally driven to a dynamically driven climatic regime.

Wright et al. (2017) described an important physical process for understanding how deforestation affects the southern Amazon rainy season using different remote sensing products. They showed that the interactions among land surface processes, atmospheric convection, and biomass burning can modify the timing of rainy season onset. These interactions precondition the atmosphere for regional-scale deep convection, which then leads to moisture convergence and consequently a rainy season onset two to three months before the southward displacement of the Intertropical Convergence Zone (ITCZ) over the region. These studies, however, either considered only qualitative information on land cover, or, when they did consider quantitative land cover data, it was fixed in time. Although this is not a problem for studies of a single season or for modeling studies, this is a significant limitation for hydroclimatic studies that analyze several rainy seasons in this region with intense land cover dynamics. A new yearly land cover and land use data set at 1-km resolution (Dias et al., 2016) now allows the exploration of explicit relationships between rainy season characteristics and deforestation extent.

Other studies have investigated the occurrence of dry spell events in several regions of Brazil and the large-scale climatic variations associated with them (Assad et al., 1993; Carvalho et al., 2000; Silva and Rao, 2002; Minuzzi et al., 2005;

Sleiman, 2008). However, Erfanian et al. (2017) argued that recent dry periods in the Amazon cannot be explained only by changes in sea surface temperature, suggesting that other factors are contributing to severe drought. Here, I also investigate the relationship between deforestation and dry spells in the region.

This study has two main goals. First, I revisit the relationship between rainy season onset and the scale of deforestation in southern Amazonia using the yearly land use data of Dias et al. (2016). Second, I evaluate the relationship between the scale of deforestation and the duration of dry spells occurring during the rainy season (September to April). Both analyses provide relevant information to the local agricultural sector.

1.2. Data and Methods

1.2.1. Region studied

The area studied is southern Amazonia, which ranges from 6°S to 14ºS latitude and from 65ºW to 51ºW longitude and includes the state of Rondônia, southern Amazonas, northern Mato Grosso, and southwestern Pará (Figure 1.1). This region was selected because it possesses five characteristics fundamental for the study: (1) rain that is typically convective (Marengo, 1995); (2) strong coupling between forest and climate (Fu et al., 2013); (3) strong rainfall seasonality, with well-defined dry and rainy seasons (Marengo, 2004; Davidson et al., 2012); (4) considerable albedo differences between native vegetation and deforested areas (Culf et al., 1996); and (5) intense deforestation in the past several decades (Dias et al., 2016). These characteristics are expected to facilitate the detection of a relationship between deforestation and the rainy season.

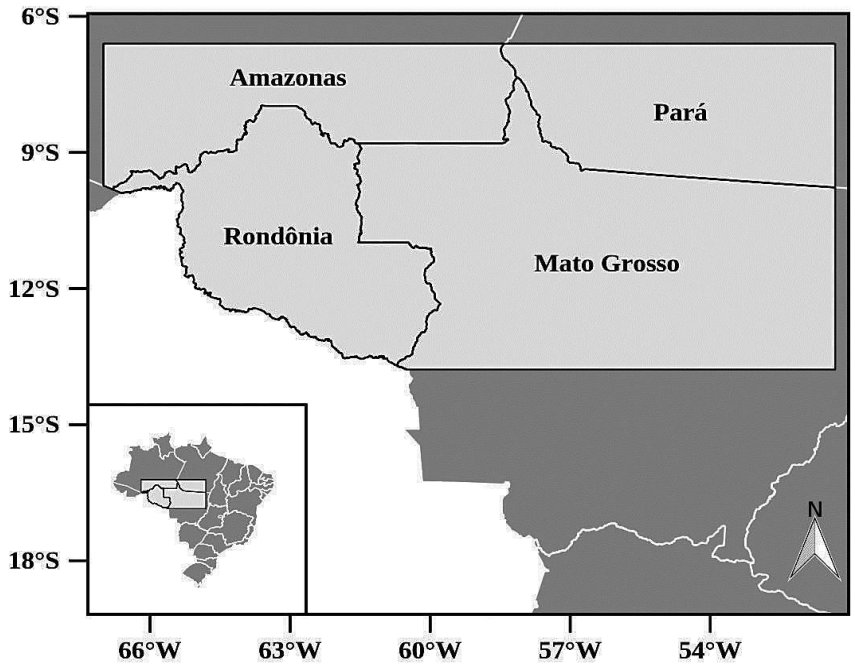

Figure 1.1. Location of study region within Brazil.

Containing the major part of the arc-of-deforestation (Ferreira et al., 2005), this region has been the center of major and rapid deforestation activities in the Brazilian Amazon since the 1970s, having areas with a large range of spatial scales of deforestation. Changes in land cover from 1970 to 2012 within the study area affected 191,319 km² (Dias et al., 2016), or 48.2%, of the total deforestation by 2012 in the Amazon (396,850 km²; INPE, 2012).

The historical causes of deforestation in this region include predatory exploitation of forests for timber (Nepstad et al., 2001) and infrastructure expansion, such as road building and urbanization (Carvalho et al., 2001; Laurance et al., 2001). Later, expansion of cropland (especially soybeans) and pastureland became major driving forces (Morton et al. 2006; Macedo et al., 2012; Dias et al., 2016).

1.2.2. Land cover data

I used the land use database developed by Dias et al. (2016) [available at: www.biosfera.dea.ufv.br/en-US/banco/uso-do-solo-agricola-no-brasil-1940-2012---dias-etal-2016] as our main source of land cover data. This historical reconstruction provides the longest agricultural land cover and land use database currently available for this region. These data were produced from a combination of yearly remote sensing data (Hansen et al., 2013), which provided the locations of forest cover, and agricultural census data, which provided the link between deforested areas and agricultural land use. The results were then aggregated at 30″ spatial resolution (approximately 1 km × 1 km). The final data are in hectares per pixel, which for our analysis were converted into percentages of deforested land per 1-km^2 pixel.

I calculated the ratio of deforested area within different spatial scales based on the concept of buffer zones, similarly to Debortoli et al. (2015). This approach consists of using three circular buffer zones centered on the coordinates of each rain gauge station, with radii equal to 20, 25 and 30 km (Figure 1.2). Defining buffer zones of fixed sizes allowed the calculation of the deforestation fractions in each year and the calculation of correlations between specific rainy season properties and deforestation fractions at different scales.

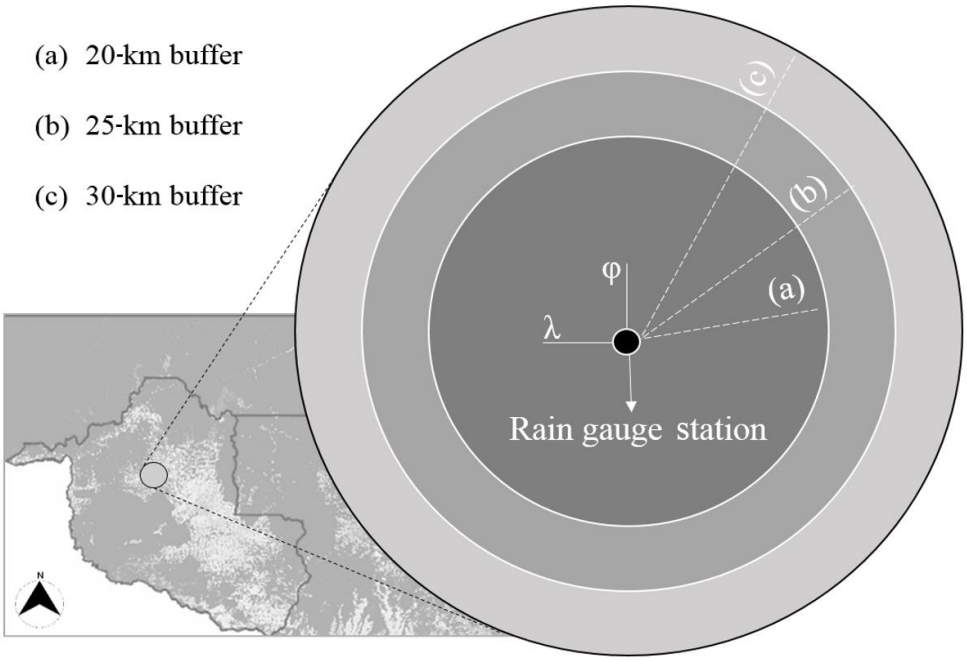

Figure 1.2. Illustration of the applied methodology showing an example of three buffer zones of differing radii surrounding a single rain gauge station: (a) 20 km, (b) 25 km, and (c) 30 km. The percentage of deforested land in each of these zones was analyzed in relation to the associated rain gauge data. Rain gauge station locations are identified by latitude (φ) and longitude (λ).

1.2.3. Rainfall data

I analyzed daily rainfall data from 112 stations across the region, covering the period from 1974 to 2012, which I obtained from the Hydrological Information System of ANA (Brazil's National Water Agency) [*HidroWeb, http://hidroweb.ana.gov.br/*, accessed 2016] (Figure 1.3). Of these time series, sixty cover more than 20 years and fifteen cover more than 30 years (Appendix A, Table A1).

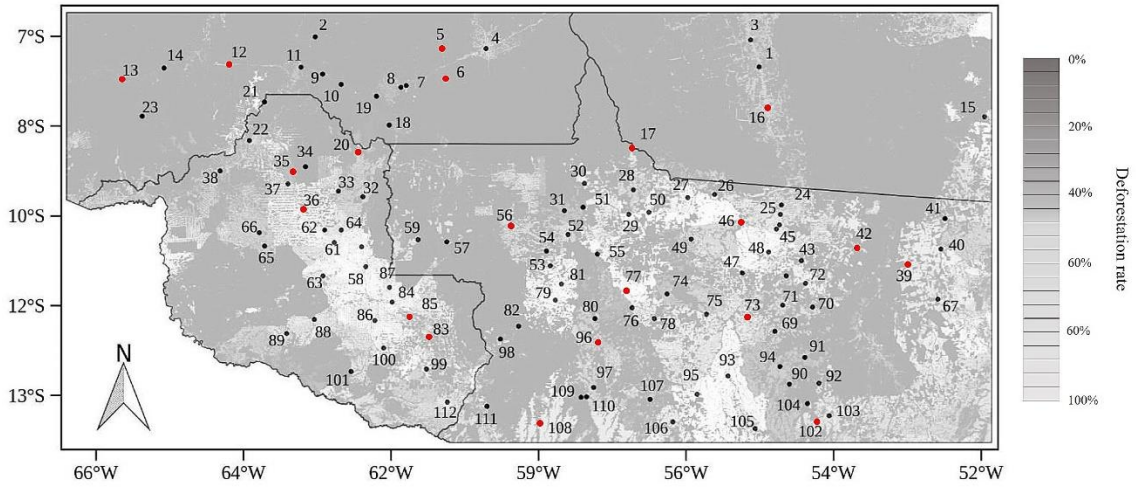

Figure 1.3. Distribution of rainfall stations in the region studied in relation to areas of deforestation in the year 2012. Light gray pixels represent areas deforested in 2012. Rainfall stations represented in red provide time series longer than 25 years.

I performed quality control procedures on the rainfall data used in my analysis. For each rainfall station, I completely eliminated any years of the time series that met one or more of the following three criteria: (1) they included daily precipitation values greater than 350 mm (I considered these to be either measurement errors or rare extreme events that I eliminated from the analysis to avoid biases; Fetter et al., 2018); (2) they presented a sequence of equal daily rainfall values for seven or more days (e.g., exactly 10 mm every day for nine days), indicating possible measurement errors; or (3) they included one or more missing data points between 1 September and the onset of the rainy season for that hydrological year.

1.2.4. Identification of rainy season onset and dry spells

The rainy season (period of strong convective activity) in the Amazon comprises the months of November through March, and the dry period, May through September (Figueroa and Nobre, 1990; Marengo, 1995). In this study, to encompass

the annual transition period between the dry season and the rainy season (September and October), the period of analysis begins in September of each year and ends in April of the following year.

Several methods have been developed to identify rainy season onset dates in tropical regions (Stern and Coe, 1982; Sugahara, 1991; Marengo et al., 2001; Odekunle and Buyiro, 2003; Liebmann et al., 2007; Liebmann and Mechoso, 2011; Butt et al., 2011). Stern and Coe (1982) defined rainy season onset as the first day on which precipitation is equal to or greater than 20 $mm \cdot day^{-1}$ for two or three consecutive days if there is no period of seven or more days with zero precipitation in the following month. Oliveira et al. (2000) adopted this method for estimating planting dates for rice in the Brazilian state of Minas Gerais with good agreement to observed dates. More recently, Butt et al. (2011) defined rainy season onset in the Brazilian state of Rondônia as the first day after 1 September (inclusive) when daily precipitation exceeds 20 mm.

Following Stern and Coe (1982), I defined rainy season onset ($B_{i,j,t}$, where "B" stands for "beginning") as the first day after 1 September (inclusive) that has daily precipitation greater than 20 mm followed by at least one more rain event (daily precipitation more than 1 mm) in the subsequent seven-day period. The subscripts i, j, and t refer to latitude, longitude, and year, respectively. The dates were indexed so that 1 September becomes "Day 1," 2 September is "Day 2," and so on.

The definition of a dry spell ($DS_{i,j,t}$) varies among studies according to the objectives in each case (Sharma, 1996; Ceballos et al., 2004; Soares and Nóbrega, 2010). In this study, I defined $B_{i,j,t}$ and $DS_{i,j,t}$ based on agricultural criteria, since our interest relates to the importance of rain for rainfed agriculture in the region. A dry spell is an event characterized by a minimum of eight consecutive days with daily

precipitation less than 1 mm and starting after $B_{i,j,t}$, as previously defined. This represents a drought interval potentially damaging to crops and is similar to the definition of Assad and Sano (1998).

The $DS_{i,j,t}$ duration is calculated in days and is classified according to the month in which a $DS_{i,j,t}$ event starts. For example, if a dry spell event begins on 28 September and ends on 13 October, the starting month is September. Next, I divided the rainy season into an early rainy season (SO, including the months of September and October, post-onset), a peak rainy season (NDJF, including November, December, January and February), and a late rainy season (MA, including March and April).

1.2.5. Anomalies in rainy season onset

There is a precipitation seasonality gradient across the Amazon, and consequently, geographical position affects rainy season temporal parameters (Costa and Foley, 1997; Sombroek, 2001; Marengo et al., 2001; Gan et al., 2004; Butt et al., 2011). Therefore, I based our analyses on the anomalies of the $B_{i,j,t}$ values ($B'_{i,j,t}$), removing the signal of the geographic position and the interannual variability (which reflect the effects of large-scale mechanisms) to find evidence of the deforestation signal. To calculate these anomalies, first I estimated the parameters of the linear equation that describe the best-fit linear regression relationship between $B_{i,j,t}$, latitude (φ), and longitude (λ). The resulting geographical trend is explained by Equation 1.1,

$$\hat{B}_{i,j} = 30.44 - 0.97\varphi + 0.29\lambda \quad \text{(Eq. 1.1)}$$

where negative values of latitude indicate locations south of the equator, and negative values of longitude refer to locations west of the Greenwich meridian. I

then calculated the onset anomalies ($B'_{i,j,t}$) by subtracting the geographical trend and the annual averages (mean anomaly at all stations for a specific year) (Equation 1.2):

$$B'_{i,j,t} = (B_{i,j,t} - \widehat{B}_{i,j})_{i,j,t} - \overline{(B_{i,j,t} - \widehat{B}_{i,j})_t} \text{ (Eq. 1.2)}$$

1.2.6. Data analysis

Initially, to demonstrate the gradient of onset of the rainy season ($B_{i,j,t}$) across the entire study area, I constructed $B_{i,j,t}$ maps for 1985, 1995, and 2005. I interpolated $B_{i,j,t}$ data from rain gauge stations using the kriging method and estimated sample variograms. Next, I fitted $B_{i,j,t}$ with a Gaussian spherical model (Pebesma, 2004; Pebesma and Heuvelink, 2016).

To consider the correlation between deforestation and time, separating the effects of deforestation from the mean long-term trend in $B_{i,j,t}$, I performed *t* tests to compare the onset of the rainy season between stations without significant change in their deforestation fraction over time and stations that experienced increasing deforestation within the 25-km buffer. For this, I subsampled 20 stations spatially distributed in the region (Represented in red in Figure 1.3)) that provided time series longer than 25 years and divided them into two groups (Table 1.1).

Table 1.1. Selected stations that provided time series longer than 25 years, and groups divided by deforestation fraction in the 25-km buffer zones.

Group	Stations	Mean Latitude	Mean Longitude	Period	Mean Deforestation (%)
1	5, 6, 12, 13, 17, 35, 36, 39, 83, 85	-9.1697	-60.5167	1970s–1980s	4.1
				1990s–2000s	3.9
2	16, 20, 42, 46, 56, 73, 77, 96, 102, 108	-10.4988	-56.8653	1970s–1980s	4.2
				1990s–2000s	13.0

Next, I investigated the correlation between deforestation fraction and $B'_{i,j,t}$. For each buffer circle size, I classified the deforestation fraction into eight classes: Class 1 has < 5% of its area deforested; Class 2 has between 5% and 10% deforested; and so on, through Class 8, with between 35% and 40% deforested. I averaged $B'_{i,j,t}$ for each deforestation class and found that the means of onset anomalies $\left(\overline{B}'_{i,j,t}\right) \cdot B'_{i,j,t}$ were normally distributed (Shapiro–Wilk test, $p < 10^{-9}$, Shapiro and Wilk, 1965), thus it was appropriate to apply a linear regression model and estimate the standard error of the mean.

To compare the effects of deforestation on the frequency of dry spells of any duration, I performed *t* tests against the null hypothesis that the mean duration of $DS_{i,j,t}$ is not significantly different between two deforestation classes (0%–20% and 20%–40%) for the 20-km and 25-km buffers for three periods of the rainy season: SO, NDJF and MA.

I assigned probabilities directly based on the $B'_{i,j,t}$ and $DS_{i,j,t}$ elements according to the probability of occurrence in the sample space generated. For this, I constructed cumulative probability density functions (CDFs) of $B'_{i,j,t}$ and $DS_{i,j,t}$ divided into two contrasting classes of deforestation (0%–5% and 30%–35%), which I considered to be low and high deforestation rates, respectively. The graph of the CDFs was generated as a product.

1.3. Results

The $B_{i,j,t}$ maps revealed a northwest-to-southeast gradient in the study area (Figure 1.4d, e, and f), which has also been found in other studies (Costa and Foley, 1997; Sombroek, 2001; Vilar et al., 2009). This gradient is due to the interactions between tropical convection systems and midlatitude frontal systems leading to the appearance of the SACZ during springtime, indicating a gradual arrival of the rainy

season (from NW to SE) and corresponding to a gradual onset of the South American monsoon (Gan et al., 2004). This result reinforces the importance of controlling for the influence of geographical position in the onset data.

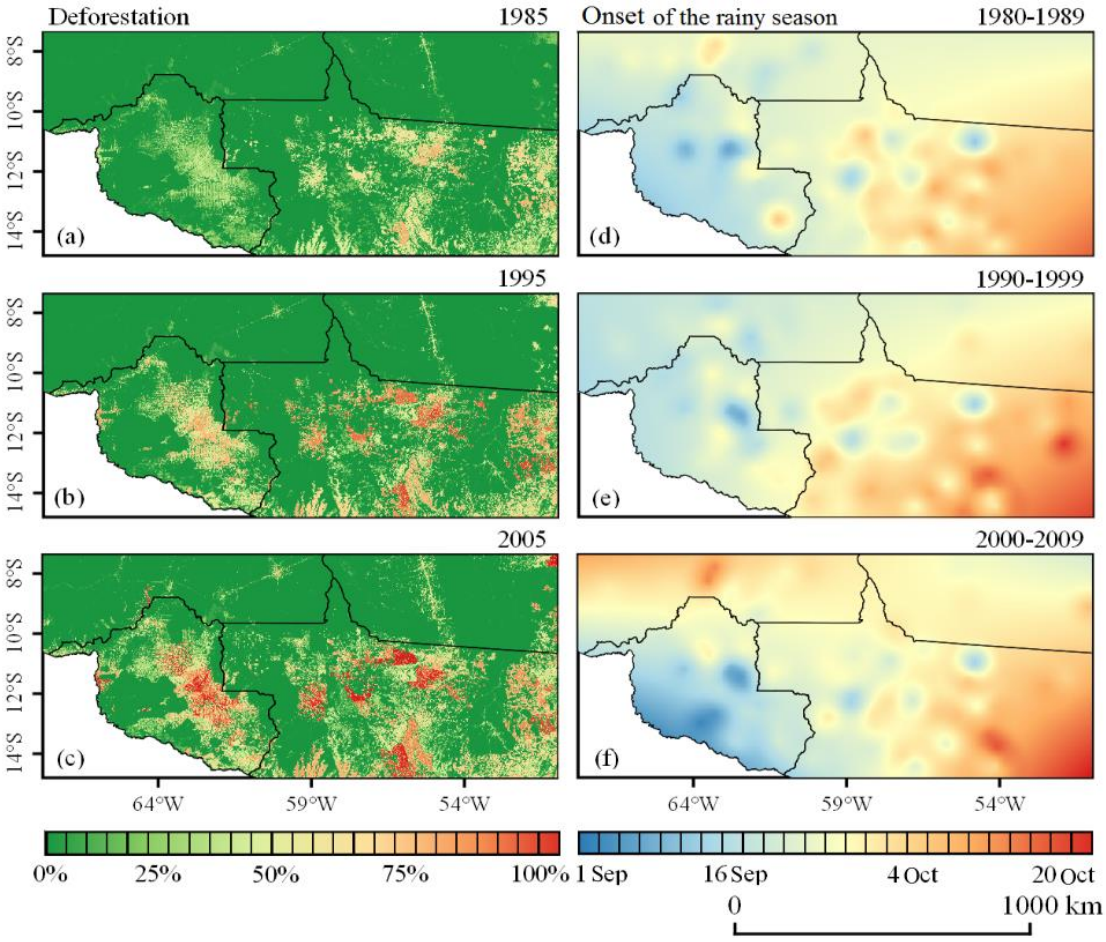

Figure 1.4. Evolution of deforestation in the region studied for (a) 1985, (b) 1995, and (c) 2005, and mean of rainy season onset dates for each of three decades: (d) 1980–1989, (e) 1990–1999, and (f) 2000–2009.

Table 1.2 displays the average of $B_{i,j,t}$ in the 1970s–1980s as compared to the 1990s–2000s for two station groups and the results of the independent two-sample *t* test. For stations within areas with increasing deforestation fractions over the years (Group 2), $B_{i,j,t}$ was delayed by about six days, whereas for stations within areas with constant land cover (Group 1), the delay was about two days.

Table 1.2. Results of the independent two-sample *t* test with unequal sample sizes and unequal variance of the means of $B_{i,j,t}$ for Station Groups 1 and 2 for the 1970s–1980s and for the 1990s–2000s (μ1970s–1980s and μ1990s–2000s).

Group	$\mu_{1970s–1980s}$	$\mu_{1990s–2000s}$	$S^2_{1970s-1980s}$	$S^2_{1990s-2000s}$	t_{calc}	$P_{1\text{-tailed}}$
1	17 Sep	19 Sep	4.6	5.1	0.351	0.347
2	18 Sep	24 Sep	4.8	5.5	-2.133	0.011

The *t*-test results indicate that for Group 2, the $B_{i,j,t}$ is significantly different between the 1970s–1980s and 1990s–2000s at the 98.9% confidence level. However, for Group 1 no significant difference in onset was found between the periods for the group with constant land cover.

Figure 1.5 shows the means of rainy season onset anomalies ($\bar{B}'_{i,j,t}$) in different deforestation classes after removing the effects related to geographical position and year, and it shows the corresponding values for standard error of the mean. The linear regressions for the 20-km, 25-km, and 30-km buffers evidence a delay in $B_{i,j,t}$ of 0.12–0.17 days per each 1% increase in deforestation. All the trends are significant at the 99% confidence level. Considering these coefficients, a deforestation rate of 50–60% corresponds to about a one-week delay in the rainy season onset. The trends evidenced differences between the three buffer sizes.

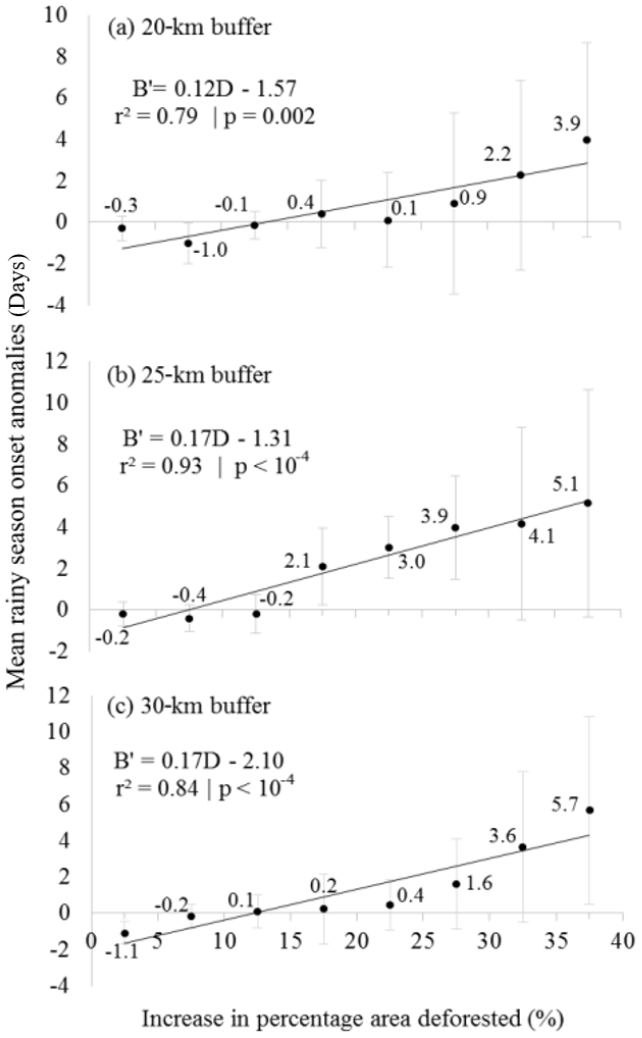

Figure 1.5. Mean of rainy season onset anomalies (days) in different deforestation classes, and standard error of the mean for the three buffer sizes: (a) 20 km, (b) 25 km, and (c) 30 km. Best-fit linear regression line and associated parameters are also shown.

Although the average of onset anomalies is representative of each deforestation class, it is also possible to calculate the probability of occurrence of $B'_{i,j,t}$ using CDFs. Figure 1.6 shows that, for the buffers larger than 20 km, in years when the rainy season starts later, there is little difference in whether a region is heavily deforested or not; in this situation, the transition from the dry season to the rainy season is probably dominated by large-scale mechanisms (which were removed from the first part of our analysis, as described above). However, in years when the

rainy season starts earlier, greater forest cover is associated with earlier $B_{i,j,t}$, since it increases the sensitivity of the system to large-scale mechanisms.

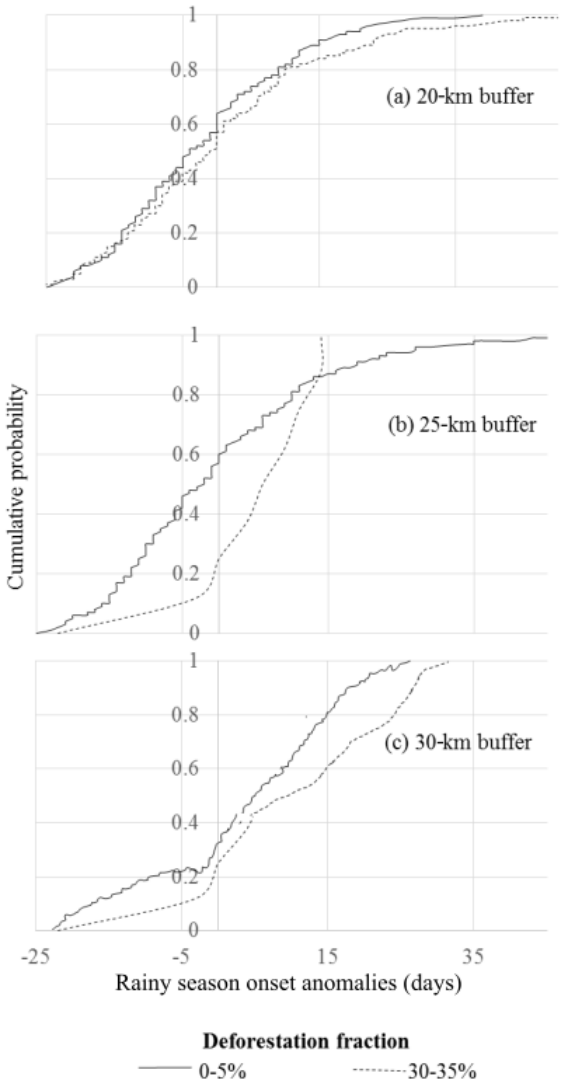

Figure 1.6. Cumulative probability density function (CDF) of the rainy season onset anomalies for three different buffer sizes: (a) 20 km, (b) 25 km, and (c) 30 km.

In addition to being able to anticipate rainy season onset dates, knowing the probability that a dry spell event ($DS_{i,j,t}$) will occur after the rainy season onset is also useful information for farmers in rainfed systems. Table 1.3 shows the results of the independent two-sample *t* test of the means of DS duration for Deforestation

Classes 1 (0–20%) and 2 (20–40%) in the 20- and 25-km buffers for three periods: SO, NDJF and MA.

The *t* test results indicate that for the SO and MA periods, for 25-km buffer sizes, the duration of dry spells was higher in the more deforested area at the 99% confidence level, and slightly less significant for the 20-km buffer size (98% confidence level). However, for NDJF, there was no significant difference in $DS_{i,j,t}$ duration between the deforestation classes.

Taking into consideration the effect of the buffer sizes studied and the spatial dimension of deforestation, I observed that there was an increased occurrence of longer $DS_{i,j,t}$ lasting between 8 and 14 days events in the 25-km buffers as compared to the 20-km buffers in SO and MA, which is not observed in the peak of the rainy season (NDJF). In other hand, for SO and MA, there was a greater number of longer $DS_{i,j,t}$ in the 20-km buffer compared to the 25-km buffer.

Table 1.3. Results of the independent two-sample *t* test with unequal sample sizes and unequal variance of the means of DS duration (μ_1 and μ_2) for Deforestation Classes 1 (0–20%) and 2 (20–40%).

Buffer size	**Period**	μ_1	μ_2	n_1	n_2	S_1^2	S_2^2	t_{calc}	$P_{1\text{-tailed}}$
20 km	SO	13.0	15.2	2258	1078	40.1	38.5	-2.0431	0.011
20 km	NDJF	11.5	10.9	947	1582	21.9	6.3	0.348	0.362
20 km	MA	13.6	14.9	2154	1586	42.7	63.1	-2.0442	0.012
25 km	SO	13.3	14.4	2193	201	7.4	8.6	-2.5945	0.003
25 km	NDJF	9.6	9.8	736	356	8.6	9.8	0.2461	0.250
25 km	MA	12.8	14.8	1945	710	22.9	9.5	-2.5847	0.008

Figure 1.7 shows the CDFs of the duration of DS events lasting eight days or longer, for 20- , 25- and 30-km buffer sizes, in two deforestation classes. For all the

buffers analyzed, the probability of occurrence (an estimate of how often a DS of equal duration occurs) of longer DS events is higher in the areas that have experienced greater deforestation (of 30–35%, by area) than in the less deforested areas (0–5% deforested), regardless of the event's duration. I also observe a more evident contrast between the deforestation curves (0–5% and 30–35%) in SO and MA (early and late rainy season) as compared to NDJF (peak of the rainy season). The more evident differences during the early and late periods emphasize when deforestation appears to make a difference.

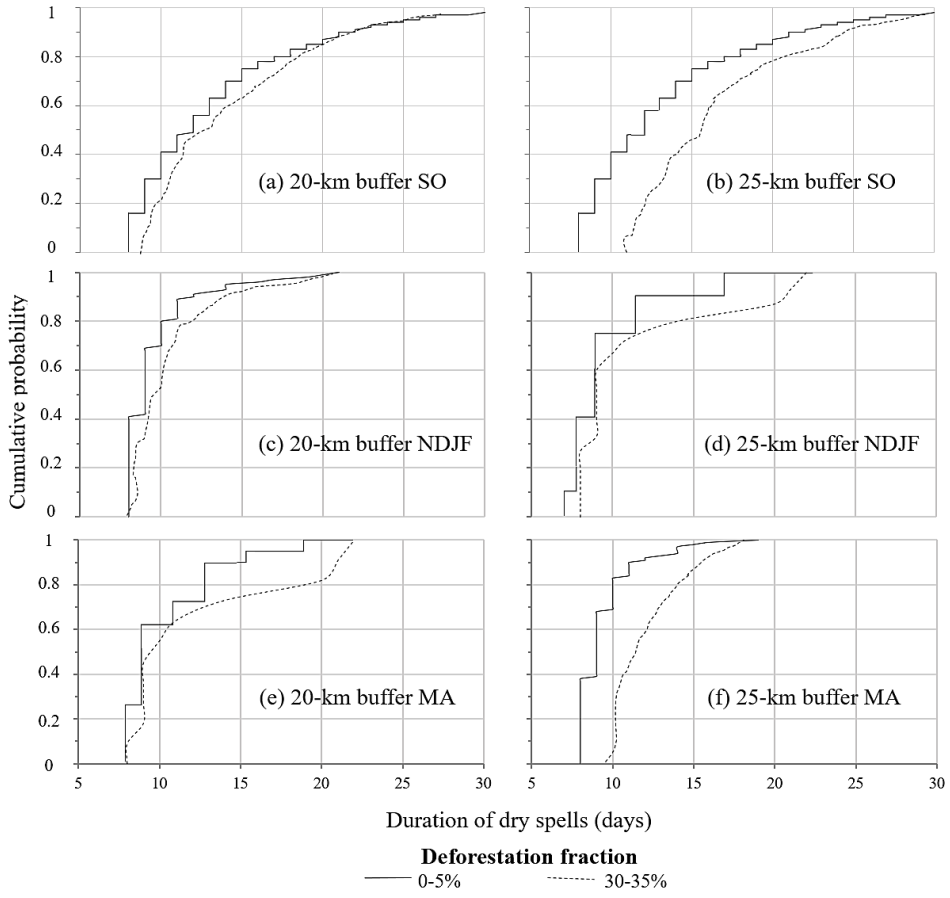

Figure 1.7. Cumulative probability density function (CDF) of the duration of dry spells for the early rainy season (SO, post-onset), for the peak rainy season (NDJF), and for the late rainy season (MA) for two different buffer sizes: (a) 20 km, SO; (b) 20 km, NDJF; (c) 20 km, MA; (d) 25 km, SO; (e) 20 km, NDJF and (d) 25 km, MA.

In SO, for the 25-km buffer, the probability of occurrence of a dry spell of ≥ 15 days in a region 0–5% deforested is about 23%, and this risk increases to about 55% in areas with deforestation between 30 and 35% (Figure 1.7b). For the same buffer size, in MA, increased deforestation also increases the probability of occurrence of a dry spell of the same duration (≥ 15 days). In areas with low deforestation, this probability is null, whereas in areas with high deforestation, the probability is 17% (Figure 1.7f).

Even if the CDFs for the peak wet season are not much different between the deforestation classes, the more evident differences during the early and late periods emphasizes that during SO and MA, deforestation appears to have made a difference.

1.4. Discussion

Although methodological differences do not allow for direct quantitative comparison with some studies, the trend toward delayed onset of the rainy season as suggested by our linear regressions can also be found elsewhere in the literature (Costa and Pires, 2010; Butt et al., 2011; Debortoli et al., 2015; Debortoli et al., 2016). Butt et al. (2011) used a definition of onset very similar to the one used in this study, but they did not quantitatively analyze the effect of deforestation. They found delays of as much as 0.6 days per year in the state of Rondônia; this equates to 18 days over the 30 years of their analysis, during which about 22% of the state was deforested. It is possible that the reason the rainy season onset delay identified in our study is smaller than their result is because I controlled for most of the effects associated with trends in large-scale hydroclimate mechanisms, leaving only the deforestation effect. Of the 38 stations in our study with more than 25 years of data, 65% have exhibited delayed rainy season onset. Similarly, Debortoli et al. (2015) reported onset delay in 63% of the time series analyzed for the southern Amazon.

The increase in deforestation impact with increased buffer size may be associated with different sizes of convective cells affecting deep cloud development over the buffers studied. The rain gauge data, however, is not sufficient for more solid conclusions on this matter, and high-resolution radar data would be required. Operational meteorological radars are unfortunately not available in this region.

In southern Amazonia, regional high humidity originating in the rain forest provides latent heat fluxes that promote convection. Deforestation affects energy partitioning, decreasing the latent heat flux and causing a drier-than-usual atmosphere, thus delaying the onset of the rainy season (Schubert et al., 2004). These results are also consistent with the shallow convection moisture pump (SCMP) mechanism proposed by Wright et al. (2017). At the scale of the buffers studied (mesoscale), complete or partial clearance of forest affects transpiration and weakens the conditions that promote surface convection, moistening and destabilizing the atmosphere, until finally causing a delay in the onset of the rainy season.

In some cases, especially in drought years, delays of these magnitudes in rainy season onset could jeopardize double-cropping systems as deforestation at these levels spreads (Spangler et al., 2017; Abrahão and Costa, 2018). For double-cropping systems (here, typically soybean followed by corn) to be viable, farmers need to ensure that the soybeans are harvested in time for the second crop to mature while climatic conditions are still favorable. Delays in rainy season onset may lead to a reduction of areas and years where double-cropping systems will be feasible with low climate risk.

In addition, the higher probability of longer DS events in areas that are more heavily deforested may lead to water deficit and have consequent negative effects on agricultural production, depending on the cultivar and its stage of development. This

relationship between DS events and agricultural problems has already been widely investigated (Carvalho et al., 2000; Barron et al., 2003; Silva and Rao, 2002; Soares and Nóbrega, 2010; Adekalu et al., 2009; Barron and Okwach, 2005; Fox and Rockstrom, 2003; Hernandez et al., 2003; McHugh et al., 2007).

Water deficit has a direct effect on final crop production, which depends on the crop and its stage of development (Doorenbos and Kassam, 1979). This has been demonstrated in studies such as Espinoza et al. (1980), which showed reductions of up to 60% in maize yield when dry spells occurred between the flowering stage and the grain filling stage, and Espinoza (1982), which found yields for irrigated soybean higher by 24% to 55% compared to crops experiencing water deficiency.

Occurrence of longer DS events (more likely to occur in more deforested areas) during the period of crop growth is a serious risk to agricultural production, since, as plants develop, the need for water increases and reaches maximum demand during flowering and grain-filling stages, after which the need decreases. Many consecutive dry days could exacerbate soil moisture deficits, interrupting consistent resupply of soil moisture to crops, affecting the amount of water available to the plants, and reducing agricultural yields (Doorenbos and Kassam, 1979).

In particular, I find that differences in dry spell CDFs between the two deforestation classes are only significant in SO, when the rainy season typically begins, and MA, when the rainy season typically ends. These results may be sensitive to the definition of rainy season onset used. Short-lived rain events caused by the passage of cold fronts or other synoptic-scale systems may confound the identification of the rainy season onset. Similarly, the differences in MA might imply earlier, more abrupt end of the rainy season over deforested regions.

This analysis has direct applications to agricultural planning and decision-making. In terms of risk to agriculture due to weather conditions, if farmers choose

to plant a single crop based on the presented results, they will benefit from waiting for a more secure scenario to start sowing the crop. The secure scenario is one that minimizes the probability of being affected by either delay in the onset of the rainy season or occurrence of extreme weather phenomena, such as dry spells of higher durations. A good choice of sowing season tries to match the needs of the crop during all of its developmental stages with times when favorable climatic conditions are most likely. In the case of soybeans, the sowing time should coincide with the period of the year when the water stored in the soil is most likely to be found in sufficient quantity for seed germination and seedling emergence, and therefore the establishment of the field crop; this sowing window may happen earlier in less deforested sites. These inferences are generic for the region; for farms that are located farther north in the study region, the rainy season is expected to start a few days sooner than in the southernmost part of the region.

1.5. Conclusions

This research disentangles the complicated relationship between deforestation and precipitation in southern Amazonia. By removing regional trends and interannual variability, our results demonstrate that increased deforestation contributes to delayed onset of the rainy season. For all scales analyzed, correlation analysis shows increasingly delayed rainy season onset through time as deforestation progresses. Analysis of cumulative probability density functions for rainy season onset indicates that in years that the rainy season starts earlier, the absence of forest cover delays the onset of the rainy season. In addition, a higher percentage of deforestation is also associated with a higher frequency of long dry spell events during the early and late rainy season as compared to minimally deforested regions. Land use changes happening in the study area may be imposing strong physical

changes that affect the amount of potential energy available for moist convection. These changes are due to latent heat and albedo alteration occurring in response to surface changes, and have, in turn, been influencing rainy season duration (Fu et al., 1999; Dubreuil et al., 2012; Fu et al., 2013).

The increased deforestation also increases climate-related risks to agriculture in southern Amazonia. Specifically considering the double-cropping system practiced in the region, a delay in the onset of the rainy season may limit the feasibility of growing two successive crops. It is also important for the selection of cultivars to be planted by farmers in rainfed systems, since cultivars characterized by a long juvenile period and cultivars of medium and late maturation poorly tolerate late sowing due to delayed onset of the rainy season or longer dry spell events—events which I have demonstrated are more likely to occur in areas of greater deforestation. In addition to providing information to support crop management and planning, such information is also a tool with great potential for analysis by the insurance market, and it may also be important for the development of regional policies on deforestation controls.

CHAPTER 2 - THE SOUTHERN AMAZON RAINY SEASON: THE ROLE OF DEFORESTATION AND ITS INTERACTIONS WITH LARGE-SCALE MECHANISMS.

2.1. Introduction

The southern Amazon is one of the most rapidly developing agricultural frontiers in the world, having experienced high rates of conversion of forest to croplands and pasturelands (Salazar et al., 2007; INPE, 2014). Previous studies have demonstrated that this intense land use change affects the regional precipitation (Lean et al., 1996; Costa and Foley, 2000; Davidson et al., 2012; Debortoli et al., 2015; Leite-Filho et al., 2019). These impacts are potentially important for the region, as some of its main economic activities, including agriculture, are highly dependent on climate (Sumila et al., 2017).

Southern Amazon, here in this paper defined as the region between 7°S and 14ºS

latitude, is also the transition between a wet climate with a short (1-2 months) dry season in the northern border, and a seasonal climate with a 5-6 months dry season in the southern border. In addition to the geographical position, the rainy season length and the transition between the dry season to the rainy season (onset of the rainy season) also presents significant interannual variability, which have been associated to large-scale climate mechanisms, such as anomalies in the sea surface temperature and the position of the southern hemisphere tropical jet (Yin et al., 2014). Recently, Espinoza et al. (2018) have demonstrated that the frequency of dry days has increased significantly in the region (particularly between September and November), increasing the dry season length, associated with a reduction of deep convection over southern Amazonia related to the large-scale atmospheric circulation features.

A second line of studies addressed the correlation between onset, demise and length of the rainy season and land use changes. Deforestation has been associated with delays of the onset (Butt et al., 2011, Debortoli et al., 2015, Leite-Filho et al., 2019), earlier demise (Debortoli et al., 2016) and shortenings of the length of the rainy season (Wright et al., 2017). These two independent lines of cause-effect relationships suggest that first, both may be relevant, and second, an interaction between large-scale and local effects should be investigated.

The effects of deforestation on the duration of the rainy season in the Amazon have also been investigated extensively by modeling studies. Costa and Pires (2010) verified an increase from 5 to 6 months in the length of the dry season and a delay in the onset of the rainy season in the Amazon arc-of-deforestation associated with progressive deforestation.

Deforestation affects rainfall through modifications in the surface energy flux and

injections of water vapor into the atmosphere. The substitution of a tropical forest by croplands or pasturelands increases the surface albedo and the Bowen ratio, reduces surface roughness and leads to an effectively lower soil moisture storage capacity, as the new vegetation generally has shallower root systems. It has been demonstrated that the dry season Bowen ratio is a key predictor for the onset timing (Fu and Li 2004). In addition, cleared land may have a latent heat flux 30% lower than forested land (Gash and Nobre, 1997), and reduced latent heat flux means that stronger moisture transport and deeper convection are needed to trigger rainfall. The rainforest higher rates of evapotranspiration during the late dry season helps to initiate a chain of atmospheric processes that hastens rainy season onset by 2–3 months before the arrival of the Intertropical Convergence Zone (ITCZ) over the southern Amazon (Li and Fu 2004, Wright et al., 2017).

Using 16 historical precipitation series in the Brazilian state of Rondônia between 1961 and 2008, Butt et al. (2011) demonstrated that the onset in deforested areas has delayed by 11 days on average (and up to 18 days) in the last three decades. Although deforestation has been increasing in the region during the period of study, these authors have not considered quantitative deforestation information and did not consider neither the effects related to geographical position nor trends in large-scale drivers of the interannual variability in the trends of onset of the rainy season.

Debortoli et al. (2015) demonstrated a later onset and an earlier demise of the rainy season with consequently reduced length of the rainy season in 88% of the 200 rain-gauges analyzed in the southern Amazon between 1971–2010. For the same region, Debortoli et al. (2016) found larger impacts of deforestation on the demise than on the onset of the rainy season (75% and 61% of the 200 rain-gauges analyzed, respectively). Their results also indicated that 79% of the rain-gauges had a shorter

rainy season length. Recently, Leite-Filho et al. (2019) demonstrated a delayed rainy season onset in 65% of the 38 rain-gauges with more than 25 years of data analyzed in Southern Amazon. They indicated a delay on the onset of the rainy season of 0.12–0.17 days per percent increase in deforestation in the southern Amazon, emphasizing that the likelihood of rainy season onset occurring earlier than normal decreases as the local deforestation fraction increases.

It is important to highlight here that the rain-gauge network in Amazonia is sparse and sometimes have extensive missing data in their historical series, which is a serious problem for assessing trends in rainy season. In addition, meteorological stations are usually close to cities and roads, which are typically deforested areas, making comparisons between these areas and purely forested regions difficult. Moreover, previous authors considered fixed maps of deforestation in time, neglecting the strong evolution of deforestation during their period of study. The use of remote sensing rainfall products increases substantially the amount of data to be analyzed. This enhanced data availability is crucial both to represent the spatial trends in the region and to obtain the relationships that can isolate the effects of deforestation and the interactions between deforestation and large-scale processes.

Although there are indications that both large-scale (SSTs, jet stream) and local-scale (deforestation) processes affect the onset, demise and length of the rainy season in southern Amazonia, these interactions have not been deeply studied partially because of the sparseness of the rain-gauge network in the region and the lack of long-term high-resolution maps that represent deforestation in the region. This chapter aims to detect and quantify changes on the onset, demise and length of the rainy season in the southern Amazon and their relationship to deforestation, using long-term daily remote sensing products of precipitation and yearly land-use data. I

also investigate the role of the Southern Hemisphere subtropical jet, sea surface temperature conditions and their interaction with deforestation in predicting the interannual variability of the rainy season onset.

2.2. Data and Methods

2.2.1 Region of study

Our definition of the Southern Amazon covers ~35% of Amazonia, ranging from 7°S to 14ºS latitude and from 66ºW to 51ºW longitude, comprising the Brazilian States of Rondônia, southern Amazonas, northern Mato Grosso, and southwestern Pará (Figure 2.1a).

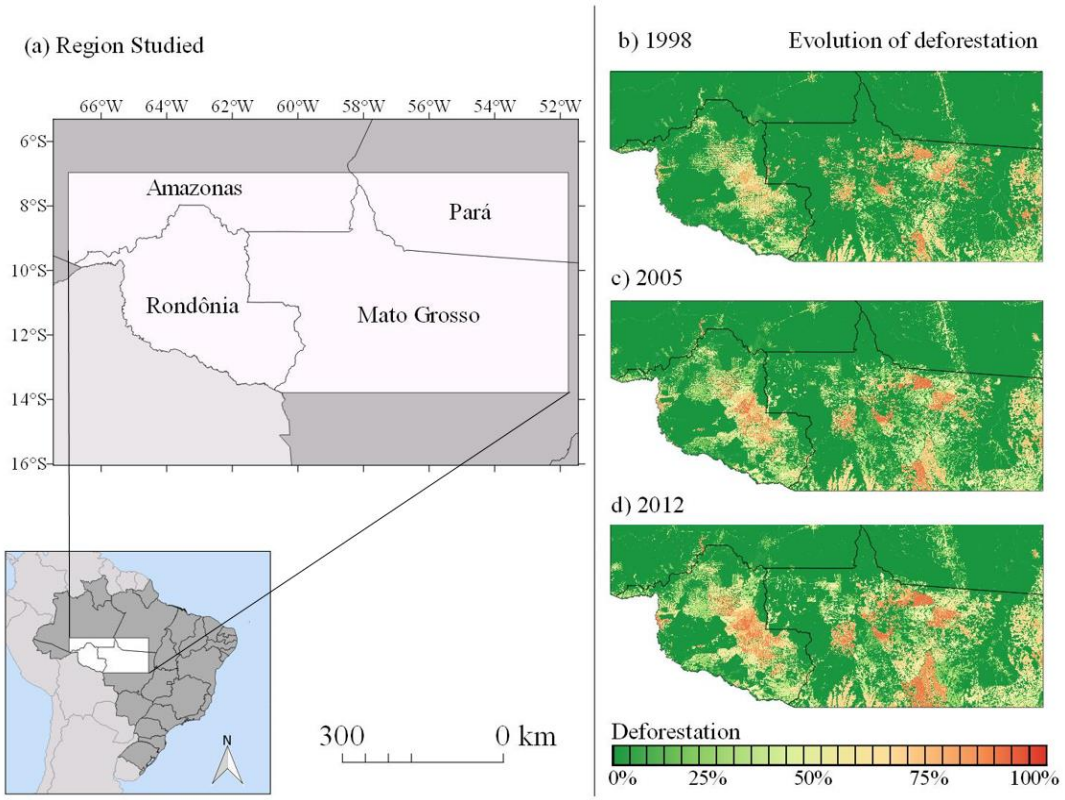

Figure 2.1. Location of studied region within Brazil and evolution of deforestation. (a) Southern Amazon, (b) Deforestation in 1998, (c) Deforestation in 2005 and (d) Deforestation in 2012.

The evolution of deforestation from 1998 to 2012 in the region is shown in Figure 1b-d, using data from Dias et al. (2016), described below. In the last decades, southern Amazonia has been an important expansion frontier for grain production and cattle ranching driven by the international commodities market (Verburg et al. 2014a, b). The agricultural expansion associated with the exploitation of timber, road expansion and accelerated urbanization have led to rapid deforestation (Leite et al., 2011). In our study period (from 1998 and 2012), data from Dias et al. (2016) indicates that more than 82,260 km² of tropical rainforest were deforested in the area. Cropland and pastureland areas increased by 26,125 km² and 56,138 km², respectively. Today, pasture remains the largest land use in the region, but its rate of growth was outpaced by the recent, rapid growth of row crop agriculture, particularly in the state of Mato Grosso (Barona, 2008, Dias et al., 2016).

2.2.2. Data

I use the Brazilian Historical Agricultural Land Use database developed by Dias et al. (2016) (available at http://www.biosfera.dea.ufv.br/en-US/banco/uso-do-solo-agricola-no-brasil-1940-2012---dias-et-al-2016), the longest agricultural land use database currently available for this region. This historical reconstruction was produced based on a combination of remote sensing data and agricultural census data. The base of the reconstruction method are the yearly maps provided by Hansen et al. (2013) that contain tree cover in each pixel from 2000 to 2012. Dias et al. (2016) mathematically combined the inverse of the tree cover maps with the agricultural census data provided by the Brazilian Institute of Geography and Statistics (IBGE – *Instituto Brasileiro de Geografia e Estatística*) and the Institute of Applied Economic Research (IPEA – *Instituto de Pesquisa Econômica Aplicada*) to

reconstruct the total agricultural land use in each pixel for each year between 1940 to 2012. These maps were originally constructed at 30″ spatial resolution (~1 km x 1 km), but in this study they are aggregated to a 28-km x 28-km grid to match the precipitation data. The final data are in hectares per pixel, which for our analysis were converted into percentages of deforested land per pixel.

I also use the daily rainfall database from the Tropical Rainfall Measurement Mission (TRMM) algorithm 3B42 version 7, for the period between September 1st 1998 to August 31st 2013, a period of 15 hydrological years. The data were extracted as NetCDF images with spatial resolution of 0.25°×0.25° (~28 km x 28 km).

I estimate that there are 9.2 M daily data points of rainfall in the study region during the period of study (7° x 15° x (4 pixels/°)^2 x 15 yr x 365 days/yr). On the other hand, considering only the continuous rain-gauge time series, there are 112 rain-gauges inside the study region, with a total of ~770,880 valid daily data points over an average of 18.8 years.

2.2.3 Identification of rainy season onset, demise and length

The transition from dry to rainy season in the southern Amazon usually occurs between the months of September and October (Figueroa and Nobre, 1990, Marengo, 1992, Hastenrath, 1997). In this study, I consider hydrological years starting on September 1st. The rainy season onset and demise dates were renumbered so that September 1st becomes "day 1", September 2nd "day 2", and so on. I used the symbols B (stands for "beginning"), E (stands for "end") and L (stands for "length") to represent the onset, demise and length of the rainy season, respectively. The symbol D is used to describe the percentage of a pixel that is deforested. The index symbols i, j and t refer to variations in the space and time dimensions.

To determine the $B_{i,j,t}$, $E_{i,j,t}$ and $L_{i,j,t}$, I use a modified version of the Anomalous Accumulation method (Liebmann et al., 2007), successfully used by Arvor et al. (2014) for the same purpose on the Brazilian State of Mato Grosso using the given gridded data used here. The Anomalous Accumulation of rainfall (AA, mm.day^{-1}) is defined at each grid point over time as:

$$AA(day) = \sum_{n=1}^{day}(R_n - R_{ref}) \qquad (2.1)$$

where R_n is rainfall at day n and R_{ref} is a reference rainfall value, both in mm.day^{-1}. Considering the agricultural applications of this study, R_{ref} was set to 2.5 mm/day, representative of a cultivar seedling's needs (Abrahão and Costa, 2018). The onset (demise) date is defined as the day of minimum (maximum) AA. Thus, B is defined as the day from which AA remains positive during the longest period found, whereas E occurs when AA reaches a maximum, i.e. after that day, AA starts decreasing (Liebmann et al., 2007). L is calculated by the difference between E and B (in days).

2.2.4 Anomalies in rainy season onset, demise and length

To remove the trends associated with geographic position, as well as the interannual variability associated with large-scale climate mechanisms, I calculate anomalies of each rainy season metric ($B'_{i,j,t}$, $E'_{i,j,t}$, and $L'_{i,j,t}$,) using a 4-step procedure, summarized by Equations 2.2, 2.3 and 2.4. First, I calculate linear regression equations to describe the relationship between $B_{i,j,t}$, $E_{i,j,t}$ and $L_{i,j,t}$ values with latitude (φ) and longitude (λ). Second, using these equations, I compute estimated values of onset, demise and length ($\widehat{B}_{i,j}$, $\widehat{E}_{i,j}$ and $\hat{L}_{i,j}$) due to geographical position. Third, I calculate the difference between raw values of $B_{i,j,t}$, $E_{i,j,t}$ and $L_{i,j,t}$ and the estimated values due to geographical position. Finally, I subtract from these values the annual averages of each variable calculated throughout the region of study ($\overline{B_t}$, $\overline{E_t}$ and $\overline{L_t}$).

$$B'_{i,j,t} = \left(B_{i,j,t} - \widehat{B}_{i,j}\right) - \overline{B}_t \qquad (2.2)$$

$$E'_{i,j,t} = \left(E_{i,j,t} - \widehat{E}_{i,j}\right) - \overline{E}_t \qquad (2.3)$$

$$L'_{i,j,t} = \left(L_{i,j,t} - \widehat{L}_{i,j}\right) - \overline{L}_t \qquad (2.4)$$

2.2.5 Preseason large-scale conditions associated with the rainy season onset

Following Yin et al. (2014), I explore the tropical sea surface temperature anomalies of region Niño4 ($N4'_t$) and Southern Hemisphere subtropical jet position (φ_{SJ}) in July as potential predicting factors for interannual variation of the rainy season onset over the southern Amazon. Niño4 anomalies are obtained from *NOAA's* National Climatic Data Center (http://www.cdc.noaa.gov/data/climateindices/list/). The latitude where 200 hPa zonal winds averaged along the Eastern Pacific-South American sector (100°W–50°W) equals 30 m/s on the equator side in July is defined as the Southern Hemisphere subtropical jet position (Yin et al., 2014). Zonal wind data are obtained from the National Centers for Environmental Prediction/National Center for Atmospheric Research (NCEP/NCAR) reanalysis (Kalnay et al., 1996).

2.2.6 Data analysis

Initially, statistical analysis is applied to correlate variables $B'_{i,j,t}$, $E'_{i,j,t}$ and $L'_{i,j,t}$ with $D_{i,j,t}$. I classified the deforestation fraction into nineteen classes: Class 1 has < 5% of its area deforested; Class 2 has between 5% and 10% deforested; and so on, until Class 19, with between 90% and 95% deforested.

$B_{i,j,t}$, $E_{i,j,t}$ and $L_{i,j,t}$ were normally distributed (Shapiro–Wilk test, $p < 10^{-5}$), so I apply a linear regression model between $B_{i,j}$, $E_{i,j}$ and $L_{i,j}$ and predictive variables $D_{i,j}$, φ and λ. $\overline{B}_t$, $\overline{E}_t$ and $\overline{L}_t$ values are also normally distributed (Shapiro–Wilk test, $p < 10^{-}$

[5]), thus it is appropriate to apply a linear regression model between $B_{i,j}$, $E_{i,j}$ and $L_{i,j}$ and predictor variable year (t) to evaluate their general time trend.

The annual anomalies data sets on each year are asymmetric and consequently not normally distributed. Thus, I calculated the correlation between $B'_{i,j,t}$, $E'_{i,j,t}$ and $L'_{i,j,t}$ and $D_{i,j,t}$ on each year using the Spearman rank correlation test (*Spearman, 1904).*

$\overline{B_t}$ values were also normally distributed (Shapiro–Wilk test, $p < 10^{-5}$), so, I analyzed how the variability in $N4'_t$ and φ_{SJt} explain the variability in $\overline{B_t}$ values through the application of a linear regression model, similarly to Yin et al. (2014). This analysis quantifies the contribution of the large-scale conditions that controls the interannual variation of the rainy season onset over the region.

$B_{i,j,t}$, $E_{i,j,t}$ and $L_{i,j,t}$ values were normally distributed and are used to estimate multiple linear regressions with predictor variables $D_{i,j,t}$, φ and λ. This analysis tests whether a bias was introduced when estimating deforestation impacts with $B'_{i,j,t}$, $E'_{i,j,t}$ and $L'_{i,j,t}$ values separated into deforestation classes.

Finally, $B_{i,j,d,t}$ values are also normally distributed, so they are used to estimate a multiple linear model with predictor variables $D_{i,j,t}$, ϕ, λ, $N4'_t$ and φ_{SJt} and the interaction between these large scale variables and deforestation ($D_t \times N4'_t$ and $D_t \times \varphi_{SJt}$). This analysis empirically estimates the contribution of the large-scale conditions to control the rainy season onset over the Southern Amazon and the complex interaction of these large-scale climatological factors with deforestation. I constructed empirical models to predict the rainy season onset in two situations: throughout the entire study region, and specifically in pixels with agricultural lands (i.e., pixels with deforestation > 1%).

I tested the statistical significance of all regression coefficients by dividing the estimated coefficient over the standard deviation of this estimate. Finally, the coefficients of sample correlation between the pairs of explanatory variables are used to detect collinear relations between two explanatory variables or between one of them and the others included in the empirical models.

2.3. Results

2.3.1 Spatial variability of onset, demise and length of the rainy season

Our rainy season maps indicate that there are zonal east–west and meridional north–south gradients of onset, demise and length of the rainy season over southern Amazonia, which is also supported by previous works (Costa and Foley, 1997, Sombroek, 2001, Nobre et al., 2009, Vilar et al., 2009, Arvor et al., 2014, Debortoli et al., 2015). For all rainy season metrics, the regression coefficients show that there is higher meridional variation (φ) than zonal variation (λ) (Equations 2.5, 2.6 and 2.7).

$$\widehat{B}_{i,j} = 12.790 + 2.438\varphi - 0.397\lambda \ (r^2 = 0.19, p < 10^{-6}) \qquad (2.5)$$

$$\widehat{E}_{i,j} = 221.786 - 5.474\varphi + 1.482\lambda \ (r^2 = 0.37, p < 10^{-6}) \qquad (2.6)$$

$$\widehat{L}_{i,j} = 145.020 - 8.703\varphi + 2.173\lambda \ (r^2 = 0.34, p < 10^{-6}) \qquad (2.7)$$

where latitudes to the south of the Equator receive negative values, and longitude west of the Greenwich Meridian receive negative values.

These regressions are represented in Figure 2.2. The rainy season begins in the first half- month of September for the northern regions, and as late as November in the southeastern part (Figure 2.2a). This northwest-to-southeast gradients of the onset

of the rainy season in Southern Amazon give support the Leite-Filho et al. (2019) results. September 7th is the average B at 7ºS and September 21st is the average at 14ºS, a difference of 14 days, with small east-west changes. These differences in climatological onset dates as large as 10-20 days are in agreement with the results found by Marengo et al., 2001 and Butt et al., 2011.

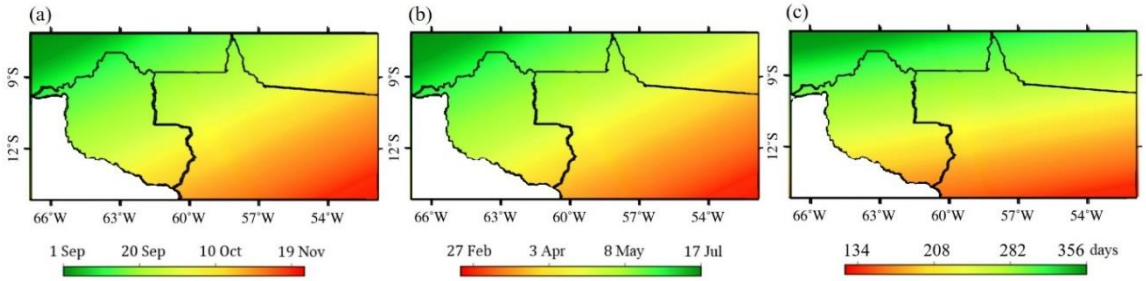

Figure 2.2. Spatial variability on the onset (a), demise (b) and length (c) of the rainy season in Southern Amazon.

Rainy season demise has a stronger dependence on longitude than the onset, although the latitude still dominates (Equation 2.6, Figure 2.2b). Rainy season ends earlier in the southeast and progressively delays northwestward (Figure 2.2b), similarly to Marengo et al. (2001). April 28th is the average of the rainy season demise at 14ºS and May 28th is the average at 7ºS, a difference of 30 days.

Rainy season length is the variable most sensitive to the zonal and meridional position (Figure 2.2c). Rainy season is shorter in the southeast and increases in length northwestward. I can verify a zonal difference ~53 days and a meridional difference ~22 days. L is strongly related to B and E as expressed by the NW-SE orientation.

2.3.2 Interannual variability and time trends of $B_{i,j,t}$, $E_{i,j,t}$ and $L_{i,j,t}$

$\bar{B}_t$, $\bar{E}_t$ and $\bar{L}_t$ are normally distributed at $\alpha = 0.05$ and exhibit clear interannual variability showed by equations 2.8, 2.9 and 2.10 and Figure 2.3. $\bar{B}_t$ has a non-significant delay of ~0.38±0.05 days per year (Equation 2.8, Figure 2.3a), corresponding to ~6±0.75 days delay along the 15 years analyzed. Although Butt et al. (2011) have used a different onset definition (first day with 20 mm rainfall), and their period of study is longer (30 years), our result (0.38 days per year) is similar to theirs (11 days of delay in 30 years, or 0.37 days per year). I find much stronger changes in $\bar{E}_t$, with a significant trend of -1.34±0.76 days per year (Equation 2.9, Figure 2.3b), or a ~20±11.74 days change in demise during the period studied. Consistently, the rainy season length decreased by 1.81±0.97days per year, corresponding to a decrease of nearly one month (~28±14.5 days) from 1998 to 2012 (Equation 2.10, Figure 2.3c). In Figure 2.3c, it is important to emphasize that the hydrological year 1997/1998 diverges significantly from the overall pattern, affecting the slope of the regression line. This outlier likely evidences a clear SST effect, since it is the stronger El Niño event in the period studied (Sampaio and Satyamurty, 1998).

$$\bar{B}_t = 0.38t - 736.97 \quad (r^2 = 0.25,\ p = 0.06) \qquad (2.8)$$

$$\bar{E}_t = -1.34t - 2947.2 \quad (r^2 = 0.44,\ p = 0.01) \qquad (2.9)$$

$$\bar{L}_t = -1.81t - 3812.4 \quad (r^2 = 0.41,\ p = 0.01) \qquad (2.10)$$

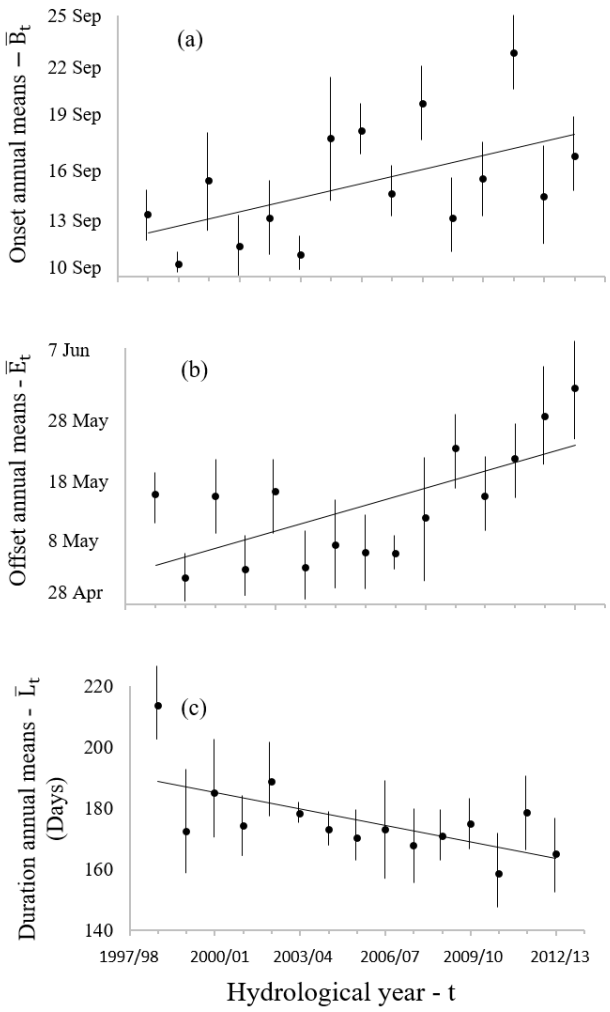

Figure 2.3. Temporal variability and annual tendency on the onset, demise and length of the rainy season in Southern Amazon (1998 to 2013). (a) onset temporal variability (b) demise temporal variability, and (c) length temporal variability. Best-fit linear regression line is shown.

Variations in the large-scale climate mechanisms that explain these rainy season variabilities in this region have been investigated in more detail by previous studies (Fu et al., 1999, Marengo et al., 2001, Ronchail et al., 2002, Yin et al., 2014). This part of the study explains how much the interannual variability of the onset can be explained by some of these large-scale preseason conditions. Equation 11 shows the resulting interannual trend between $\bar{B}_t$ with $N4'_t$ and φ_{SJt}. These two preseason conditions are significantly ($p < 0.001$) related with the onset and explains 55% of the total variance at the interannual time scale, confirming Yin et al. (2014) results.

The linkage between the Preseasonal SSTA in the tropical Pacific and rainy season onsets over the southern Amazon is consistent with studies by Marengo et al., 2001.

$$\overline{B_t} = 3.87N4'_t - 0.87\varphi_{SJt} - 4.30 \ (r^2 = 0.55, p < 10^{-5}) \qquad (2.11)$$

2.3.2. Impacts of deforestation on the onset, demise and length anomalies

$B'_{i,j,t}$, $E'_{i,j,t}$ and $L'_{i,j,t}$ are normally distributed at $\alpha = 0.05$ in each deforestation class. Equations 2.12-2.14 show the linear regressions between $B'_{i,j,t}$, $E'_{i,j,t}$ and $L'_{i,j,t}$ with deforestation. All regressions are highly statistically significant ($p < 10^{-5}$). Figure 4 shows the best-fit linear regression line and the standard error of the mean of data in each class.

$$\widehat{B'}_d = 0.04D - 4.3 \ (r^2 = 0.70, \ p < 10^{-5}) \qquad (2.12)$$

$$\widehat{E'}_d = -0.10D + 1.3 \ (r^2 = 0.73, \ p < 10^{-5}) \qquad (2.13)$$

$$\widehat{L'}_d = -0.09D - 2.4 \ (r^2 = 0.67, \ p < 10^{-5}) \qquad (2.14)$$

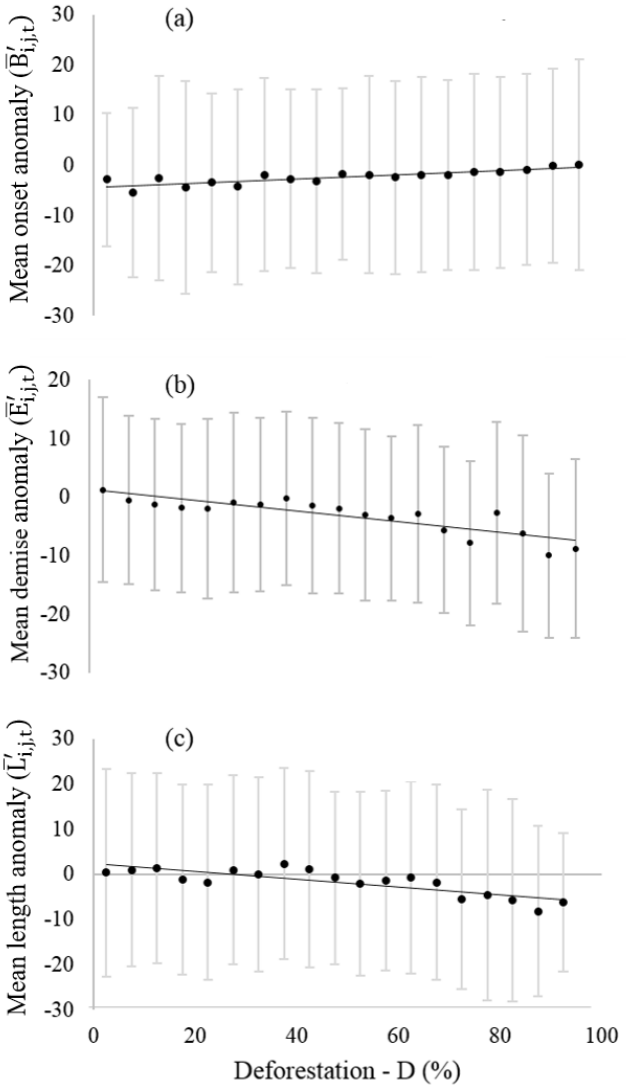

Figure 2.4. Mean of rainy season onset anomalies (a), demise anomalies (b) and length anomalies (c) in 19 deforestation classes, and standard error of the mean. The best-fit linear regression line is shown.

I find a $B'_{i,j,t}$ delay of ~0.04±0.01 days per each 1% increase in deforestation (Figure 2.4a). At the mesoscale (~ 784 km², area of the pixel studied), a hypothetical deforestation of 80% implies in an average delay of 3.2±0.8 days in $B'_{i,j,t}$, when compared to a non-deforested pixel, although there is much variability for pixels with the same level of deforestation. This higher delay on the rainy season onset in areas with greater deforestation give support the Leite-Filho et al. (2019) conclusions to the same region.

The largest impact of deforestation is observed in E, confirming Debortoli et al. (2016) results. The linear regression evidences a demise advance of ~0.10±0.02 days per each 1% increase in deforestation, after removing the effects linked to geographical position and interannual variability (Figure 2.4b). At the scale of the pixel studied, a hypothetical 80% deforestation implies in an advance of the demise of the rainy season by 8±1.6 days. Although this is a regional average for the studied region, trends are higher in southern localities, since there the rainy season ends earlier than in the northern part.

L decreases by 0.09±0.03 days per each 1% increase in deforestation (Figure 2.5c). At the scale of the pixel studied, a hypothetical 80% deforestation implies in a shortening of the rainy season by 7.2±2.4 days. I emphasize that these deforestation effects are anomalies and must be added to the annual and geographical location effects, which were removed for this analysis.

Multiple linear regressions to predict $B_{i,j,d}$, $E_{i,j,d}$ and $L_{i,j,d}$ using independent variables D_t, φ and λ (Equations 2.15, 2.16 and 2.17) indicate that the effect of deforestation (angular coefficient of D) is similar when compared to the same effect estimated using anomalies of B, E and L with respect to their geographical position (Equations 2.12, 2.13 and 2.14). The linear models explaining the demise and length anomalies through these three variables (Equations 2.16 and 2.17) have higher coefficients of determination when compared to the model explaining the onset anomalies (Equation 2.15).

$$B_{i,j,d} = 0.04D_t + 2.52\varphi - 0.43\lambda + 14.54 \qquad (r^2 = 0.18,\ p < 10^{-4}) \qquad (2.15)$$

$$E_{i,j,d} = -0.09D_t - 5.32\varphi + 1.41\lambda + 225.22 \qquad (r^2 = 0.37,\ p < 10^{-4}) \qquad (2.16)$$

$$L_{i,j,d} = -0.08D_t - 8.58\varphi + 2.12\lambda + 147.71 \qquad (r^2 = 0.33,\ p < 10^{-4}) \qquad (2.17)$$

The models so far estimate the anomaly from the long-term mean. Including $N4'_t$ and φ_{SJt} in the multiple linear models to represent the interannual variability, I estimated two geographically-explicit empirical models of the role of these large-scale mechanisms and their interactions with deforestation on the rainy season onset throughout the study region. One of the models predicts the onset of the rainy season for all pixels in the study area (Equation 2.18), and while the second one predicts the onset only in pixels with agricultural lands, i.e., areas where the deforestation > 1% (Equation 2.19).

$$B_{i,j,t,d} = 0.29D_t - 2.49\varphi - 0.43\lambda - 0.13\varphi_{SJt} - 0.51N4'_t - 0.03D_t \times \varphi_{SJt} - 0.01D_t \times N4'_t + 14.54 \quad (r^2 = 0.24,\ p < 10^{-5}) \quad (2.18)$$

$$B_{i,j,t,d} = 0.30D_t - 3.11\varphi - 0.49\lambda - 0.31\varphi_{SJt} - 0.02N4'_t - 0.02D_t \times \varphi_{SJt} - 0.04D_t \times N4'_t + 4.98 \quad (r^2 = 0.69,\ p < 10^{-5}) \quad (2.19)$$

The general model in Equation 2.18 predicts the onset of the rainy season for every pixel in the region studied, with a mean absolute error (MAE) of 7.6 days (Figure 2.5a). Containing the interannual variability predictor variables, this empirical model presents higher coefficient of determination when compared to Equation 2.15, which includes only latitude, longitude and deforestation. The relatively low variance explained in this case is an indication that there are many relevant processes may be missing in this empirical equation such as estimates of surface heat fluxes, and other large-scale processes and circulation patterns, including SSTs in other regions of the Pacific (Nino3.4 region, for example), the Bolivian High (Virji 1981) and the South American Low-Level Jet East of the Andes (Marengo et al., 2004).

However, I believe the main role is played by the surface processes. A major difference appears when a model is fit only for the pixels with agricultural lands. Equation 2.19 is a highly significant model ($p < 10^{-5}$) that predicts the space and time

variability of the onset with a MAE of 2.7 days (Figure 2.5b). Despite a slight overestimation for very low deforestation percentages, Equation 2.19 can be used as an onset forecast model for all practical purposes, given its very low MAE (2.7 days) compared to the range of variability in B across space and time (> 30 days). In addition, all regression coefficients of this empirical model are statistically significant, presenting p-value smaller than the significance level (α=0.05).

Testing the existence of multicollinearity between variables included in these models, I found that the absolute value of the correlation coefficient between all combinations of the independent variables is lower than 0.80, indicating absence of multicollinearity.

Moreover, the striking difference between the fit of Equation 2.19 versus Equation 2.18 is a strong empirical evidence of the interaction between large-scale mechanisms and deforestation. In fact, the difference between the two equations is that the former uses data for all ranges of D, including D = 0, while the latter uses data only for D > 0. Notice that, when D = 0, several terms in Equation 2.18 vanish, and this makes Equation 2.18 less fit to estimate B in 100% forested pixels.

Given the difference in statistical fit to Equation 2.19, I suggest that there are missing processes related to a non-represented spatially-varying relevant forest parameter, arguably the land surface albedo. In this sense, the percentage of deforestation considered here could be working as a proxy for the increase in albedo due to deforestation, while any spatially variability in the rainforest albedo would be missing from the empirical model. I do not discuss in depth why the fit of the general equation is not as good as the specific equation for deforested areas, which may be the subject of further studies.

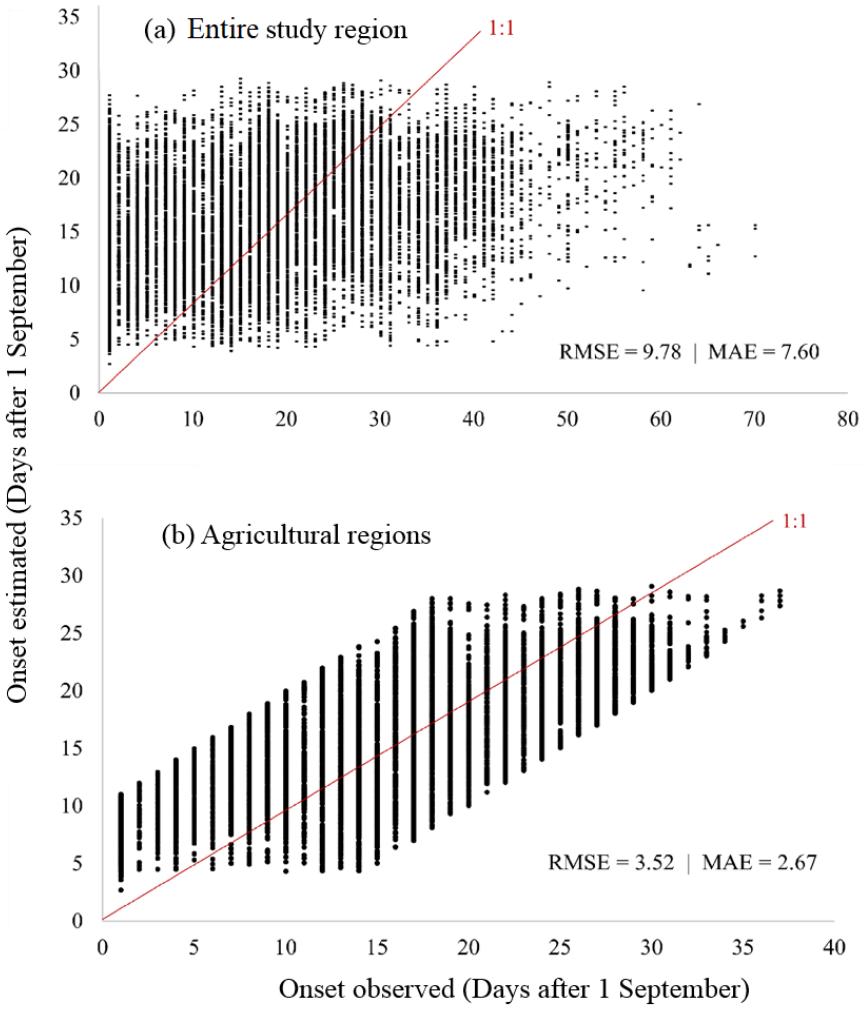

Figure 2.5. Predicted vs. observed values of onset of the rainy season compared them to the 1:1 line for (a) whole study region, and (b) agricultural regions only. RMSE is the *root-mean square error and MAE is the* mean absolute *error*.

2.4. Discussion

2.4.1. Climate dynamics

The zonal and meridional gradients of the rainy season onset and demise are mainly caused by the changes in tropical convection associated to the gradual continental heating and cooling due to changing Sun`s declination, indicating a gradual arrival and departure of the rainy season. Increased dry season length (consequently, decreased rainy season length) in southern Amazonia is related to enhanced wind subsidence (ascendance) over the 10°S–20°S (5°S–5°N) region and a

deficit of specific humidity at 1000–300 hPa south of 10°S, confirming the absence of deep convection over the region (Espinoza et al., 2018). The changes in rainy season onset and demise also affect its duration, which is also highly geographically dependent, emphasizing the importance of controlling for the geographical position in the onset, demise and length data.

Specifically, B gradient depicts the southward advance of the ITCZ, corresponding to a gradual implementation of the South American monsoon (from NW to SE) (Gan et al., 2004, Liebmann and Mechoso, 2011). This monsoon period is usually after the maximum seasonal temperature during the dry winter season. During this temperature peak, rain formation at the onset of the rainy season is very dependent on forest, which provides deep convective heating and water vapor to the atmosphere (Wright et al., 2017). A similar mechanism may explain the relationship between the forest and the demise of the rainy season.

Moreover, the rainy season is subject to strong interannual variability that is controlled by large-scale mechanisms. Trends in these large-scale mechanisms may overlap with trends in the forest cover, confounding the relationships between the causes and the changes in rainy season parameters.

By removing regional trends and interannual variability, this dependency between forest and rains was demonstrated more clearly, isolating the deforestation signal in the tendencies of onset delay, earlier demise and shortened length of the rainy season. Moreover, the deforestation effect on the onset increases when the interactions with the large-scale mechanisms are included in the empirical model. This provides empirical evidence of the relevance of the interaction between these large-scale factors with deforestation, supporting the mechanism that the onset of the rainy season in southern Amazon relies on large-scale moisture convergence aided by

local injections of water vapor and deep convective heating linked to the forest.

The higher rates of evapotranspiration of the rain forest causes an increase of shallow surface convection that moistens and destabilizes the atmosphere during the initial stages of the transition from the dry season to the rainy season. This mechanism – *Shallow convection moisture pump* (SCMP, Wright et al.., 2017) – preconditions the atmosphere at the regional scale for a rapid increase in rain-bearing deep convection, which in turn drives moisture convergence and rainy season onset 2–3 months before the complete southward shift of the ITCZ over the region.

Pastureland and soybean croplands are the main types of land conversion for agricultural use in the region. Rainforest evapotranspiration around 3.8 $mm.day^{-1}$ (Costa et al., 2010) provides sufficient moisture for localized, mesoscale convective events. The injection of water vapor in pastureland regions (1 $mm.day^{-1}$) is a much weaker source of moisture, while in cropland areas, evapotranspiration can be assumed to be zero in the weeks before crop sowing and germination. Moreover, tropical forests around 10°S in the Amazon have higher evapotranspiration rates during the end of the dry season than during the rainy season, because of higher solar radiation and higher vapor pressure deficit (Costa et al., 2010). On the other hand, pastures and croplands have a strong evapotranspiration seasonal cycle, so that differences between wet and dry season evapotranspiration are expected in deforested areas. In addition, in pastureland areas, net radiation at the surface is 6.2% less than in the rainforest, while in Soybean croplands, the decrease in net radiation is 7.0% (Sampaio et al., 2007).

The interannual variability in the rainy season metrics is also linked to interannual variations of large-scale climatic mechanisms (Fu et al. 1999, Marengo et al., 2001, Ronchail et al., 2002, Yin et al., 2014), which emphasizes the importance

of controlling the conditions of each year on the onset, demise and length variability. Two large-scale conditions are crucial for determining the interannual variability of the rainy season onset. First, a poleward shift of the Southern Hemisphere subtropical jet over the South American sector may prevent cold frontal systems from moving northward into the region. This delay of cold air incursion results in late rainy season onset over the southern Amazon. Second, El Niño episodes and SST anomalies over the subtropical south central Pacific could also influence the poleward displacement of cold fronts (Barros and Silvestri, 2002; Vera and Vigliarolo, 2000; Vera et al., 2002).

2.4.2. Agriculture and land-use implications

Brazilian agricultural production is projected to rise this century to meet part of the increasing global demand for food (OECD/FAO, 2015). To avoid negative environmental consequences, increases in Brazilian food production ideally should not be achieved by a proportional increase in the planted area, which implies in continued deforestation. The adoption of intensive agricultural techniques such as double cropping (DC) play an important role to achieve this objective. DC is a cropping system where two crops, typically soybean followed by maize, are cultivated on the same land during the same growing season. DC requires a long rainy season (> 200 days) that starts early (Costa et al., in press). So, an early sowing of soybeans is essential for farmers to ensure that the soybeans are harvested in time for the second crop to grow and mature while climatic conditions are still favorable. Therefore, DC is neither favored by a short rainy season, nor by a delayed B nor an earlier E (Arvor et al., 2014, Spangler et al., 2017, Abrahão and Costa, 2018, Costa et al., in press).

Under the Brazil's new Forest Code (Law nº. 12,651, effective since 2012), 80% of private lands in the Amazon should be protected from deforestation. Although in some cases excess deforestation can be offset in several ways defined in the legislation, in general Amazonia farmers can legally farm only 20% of their land. Considering these limits allowed by law, and according to Figure 2.4, at the 28-km x 28-km scale used in this study, the average delay in B would be only 0.8±0.20 days, the advance in E would be on average only 2±0.40 days, and L would be shorter by 1.8±0.60 days on average, which are negligible changes in the rainy season characteristics. In a larger deforestation case than allowed by law (in most of these cases deforestation happened before the approval of the current legislation), for example an extreme 80% deforestation, Figure 2.4 relationships estimate that B may delay by 3±0.80 days, E may advance by 8±1.60 days, and L could shorten by 7±2.40 days on average. Although these average changes are small (up to 5 days in duration, from the 20% scenario to the 80% scenario), they may be much larger in unfavorable large-scale scenarios.

A sensitivity analysis of Equation 2.13 shows that, in unfavorable large-scale conditions the onset of the rainy season may start significantly later. During our period of study, φ_{SJ} varied by 8°, and $N4'$ varied by 1.6 °C. Here I use the operator Δ to represent the change between favorable conditions, i.e., condition that favor an early onset of the rainy season, and unfavorable conditions, i.e., conditions that lead to a late onset of the rainy season. In unfavorable conditions like $\Delta\varphi_{SJ} = -6°$ and $\Delta N4' = -1.5$ °C, the onset of the rainy season may happen 29 days later in a 80% deforested pixel when compared to a 20% deforested pixel.

This result puts deforestation control in a new perspective. Maintaining deforestation within the permitted limit is not only a matter of obeying the law,

having more access to subsidized agricultural credit (available only to those that abide by the law) or simply not being fined. Farmers will also benefit from a rainy season that starts earlier, which reduces the risk to double cropping systems and increases farmers total crop output. In this sense, the expansion of agriculture in Amazonia may be self-defeating.

Although these results were unknown at the time the Forest Code has passed in the Brazilian Congress, they show how environmentally sensible the legislation is. Original legislators intention was to protect biodiversity, but our results show that the legislation, if strictly followed, can also help the climate regulation service provided by the rainforest, in a way that benefit the farmers that collectively (28-km x 28-km scale) respect the legislation.

Our results also encourage farmers in highly deforested regions to promote forest restoration, as localities that have high deforestation could benefit from a longer rainy season through forest restoration. Although some individual ranches in Amazonia are as large as one of our pixels (28 x 28 km, or 78,400 ha), most likely these mesoscale climate consequences will only be achieved by working as a community. In addition, the benefits of forest protection and restoration go beyond preserving the biodiversity and providing a climate more adequate to intensive agriculture, as forests provide other ecosystem services, such as sustainable extraction of timber and non-timber forest products like rubber, nuts and fruits, fire and erosion control, and carbon storage (Strand et al. 2018). The combined sustainable exploration of the forest and the possibility of a low risk intensive double cropping system expands the benefits of the high forest protection levels required by the Forest Code. Moreover, it has been suggested (Nobre et al. 2016) that the enormous biological assets of the Amazon, if preserved, could shift the economic

development paradigm of the region in the direction of creation of innovative high-value products, services, and platforms through combining advanced digital, biological, and material technologies of the Fourth Industrial Revolution in progress.

Our results also have important implications to the Brazilian government efforts to protect the country's irreplaceable forests, emphasizing the importance of public and private conservation policies, surveillance practices against deforestation, land tenure policies, land regularization and creation of innovative and efficient governance practices to mitigate socioeconomic and ecological impacts of deforestation.

2.5. Conclusions

This paper presents a quantitative connection between rainy season onset, demise and length with deforestation in the Southern Amazon, making use of temporally and spatially explicit data on land-use and rainfall. In addition, I underline the importance of the variations in the sea surface temperature and Southern Hemisphere subtropical jet position and their interaction with deforestation to determine the variability of onset of the rainy season in the region.

All rainy season metrics present a strong spatial NW-SE gradient (corresponding to a gradual implementation of the South American monsoon) and a strong interannual variability related to large-scale forcings. Particularly, Niño4 SST anomaly and Southern Hemisphere subtropical jet position in July explain 55% of the total variance of the rainy season onset at the interannual time scale.

By controlling the influences associated to geographical location and the year, I find that deforestation delays the onset, accelerate the demise, and decreases the length of the rainy season. The empirical models developed can contribute both to

understand the role that deforestation plays in the rainy season onset as rainforest continues to vanish, and to predict the rainy season onset for application in a variety of uses, including agriculture.

In summary, this study presents substantial evidence to demonstrate that land use change is a causal factor in the modifications of these rainy season metrics in Southern Amazon, while their interaction with large-scale factors must also be considered.

These results have an important role to long-term land-use regional planning and to build resilience of agriculture to climate variability. Keeping deforestation at low levels is an alternative that should be regionally considered by farmers to maintain the early onset of the rainy season, an essential climate feature in which intensive double cropping systems rely on. Depending on climate trends of key variables like Niño 4 SST and Sub-tropical Jet position, the shortening of the rainy season may jeopardize the feasibility of double cropping rainfed systems. Our results make clear the need to integrate forest conservation and restoration with agricultural practices that are directly affected by these forests.

CHAPTER 3 - GENERAL CONCLUSIONS

3.1. Dissertation overview

The work presented here is an exploratory analysis of how deforestation in southern Amazon has been causing notable changes in the hydrological cycle by altering important rainy season characteristics. In Chapter 1, I used daily rainfall data from rain gauges and a recent yearly 1-km land use database to evaluate the effects of the deforestation extent at different spatial scales on the onset of the rainy season and on the duration of dry spells. This chapter led to four main results: (I) A delay in the onset with increased deforestation; (II) The likelihood of rainy season onset occurring earlier than normal decreases as the local deforestation fraction increases; and (III) Higher occurrence of dry spells in the early and late rainy season in areas with greater deforestation (IV) Increased deforestation impact increases with increases in buffer sizes;

In Chapter 2, I evaluated the quantitative effects of deforestation on the onset, demise and duration of the rainy season using TRMM 3b42 product of precipitation

and the same land use database. Additionally, I used Niño4 anomalies and zonal wind data to explain and predict the interannual variation of the onset over the region. This step led to four main results: (I) Between 1998 and 2012 onset has delayed, demise has advanced and the rainy season has shortened; (II) Onset, demise and length have north- south and east–west gradients linked to large-scale climate mechanisms; (III) The regional seasonality seems modified by deforestation; (IV) Interannual variation of the onset in the region is explained by Niño4 sea surface temperature anomalies, Southern Hemisphere subtropical jet position, deforestation and their interactions.

3.2. Conclusions and final remarks

All two chapters presented here reported a robust signal that deforestation affects the precipitation seasonality in the southern Amazon. Onset delays, demise advances and length decreases with increasing deforestation. Within its limitations, this study also indicates that the larger the buffer area is, the deforestation impact increases. Additionally, occurrence of dry spells in the early and late rainy season is higher in areas with greater deforestation.

Particularly, the dry-to-rainy season transition period in southern Amazon appears to be directly affected by the interactions between large-scale and local-scale processes (linked to decreases in forest cover in the region). Where forest cover is replaced by agricultural lands, as is often the case of the region studied, resultant changes in the partitioning of net radiation lead to changes in the warming of the air and related evaporative processes (Bruijnzeel, 2004).

Considering that a fairly amount of water used to promote agricultural practices in the southern Amazon comes from basin-scale water recycling of the forest, changes in precipitation tend to reduce crop and pasture productivity,

increase the risk of burning in pastures or plantations, and makes the double-cropping system unfeasible. The continued unsustainable agriculture expansion, with continued deforestation in the coming years will be able to bring important impacts on the rainy season and possibly serious damage to regional agribusiness. Given this, these results contribute to reinforce the necessity of balancing agricultural development and forest conservation.

3.3. Recommendations and future challenges

Ongoing agricultural expansion in Amazonia is expected to continue over the next several decades (Morton et al., 2006) as global food demand increases (Lambin and Meyfroidt, 2011). This future scenario reinforces the importance of continuity of studies of the deforestation impacts on climate, especially in a moment that government seems favorable to the desire of agribusiness to expand pasture and intensive agriculture in the Amazon.

The coupling of the several disciplines necessary for understanding deforestation effects in the Amazon rainy season is certainly one of the major challenges faced in the upcoming years. This approach is necessary if I are to look at Amazonia and regional agriculture in a sustainable way.

Many questions are still open for debate. Future research efforts should focus on evaluating the effects of the extent of deforestation at different spatial scales on the onset, demise and length of the rainy season for more solid conclusions on this matter. A more extensive network of operational meteorological radars could more precisely test the hypothesis that the increase in deforestation size may be associated with different sizes of convective cells affecting deep cloud development.

Other large-scale variables and dynamic feedbacks not incorporated in the empirical model could ascent as strong indicators of the rainy season onset. In addition, the pattern of deforestation (concentrated versus dispersed deforestation, for example) can be investigated. It should also be relevant evaluate the relationship between the scale of deforestation and the duration of dry spells using remote sensing products.

While I find that the energy modifications is sufficient to explain the broad features of the observed changes in the southern Amazon rainy season, more work is required to quantify to what extent other processes such as changes in evapotranspiration and moisture recycling may have also contributed.

REFERENCES

ABRAHÃO, G. M.; COSTA, M. H. **Evolution of rain and photoperiod limitations on the soybean growing season in Brazil: The rise (and possible fall) of double-cropping systems.** Agricultural and Forest Meteorology, 2018. 256–257, 32–45. https://doi.org/10.1016/j.agrformet.2018.02.031.

ADEKALU, K. O.; BALOGUN, J. A.; ALUKO, O. B; OKUNADE, D. A.; GOWING, J. W.; FABORODE, M. O. **Runoff water harvesting for dry spell mitigation for cowpea in the savannah belt of Nigeria.** Agricultural Water Management, 2009. 96, 1502–1508.

ANA – **Agência Nacional de Águas**. Hidroweb, 2016. http://hidroweb.ana.gov.br (accessed September 2016).

ARTAXO, P. **Links between the terrestrial biosphere and the atmosphere: a case example in Amazonia.** In Eighth European Symposium on the Physico-Chemical Behaviour of Atmospheric Pollutants, Torino, Italy, Institute for Environment and Sustainability, Biodiversity and Global Change Unit, 2001.

ARVOR, D.; DUBREUIL V.; RONCHAIL J.; SIMÕES M.; FUNATSU B. M. **Spatial patterns of rainfall regimes related to levels of double cropping agricultural systems in Mato Grosso (Brazil).** International Journal of Climatology, 2014. 34, 2622–2633. https://doi.org/10. 1002/joc.3863.

ASSAD, E. D.; SANO, E. E. **Sistema de informações geográficas – Aplicações na agricultura.** 2.ed. Brasília: EMBRAPA-CPAC, 1998. 434p.

ASSAD, E.; SANO, E.; MASUTOMO, R.; HERNAN, R. DE C. L.; MACENA, F. **Veranicos na região dos Cerrados brasileiros frequência e probabilidade de ocorrência.** Pesquisa Agropecuária Brasileira, 1993. 28, 993-1003.

BARONA, E. **Identifying the role of crop production in land cover change in Brazil, 1990-2006.** M.S. thesis, Department of Geography, McGill University, Montreal, 2008.

BARRERA, D. F. **Precipitation estimation with the hydro-estimator technique: its validation against raingauge observations.** VII Congresso da IAHS, Foz do Iguaçu, 3-9 de abril de 2005.

BARRON, J.; OKWACH, G. **Run-off water harvesting for dry spell mitigation in maize (*Zea mays L.*): results from on-farm research in semi-arid Kenya.** Agricultural Water Management, 2005. 74, 1–21.

BARRON, J.; ROCKSTRÖM, J.; GICHUKI, F.; HATIBU, N. **Dry spell analysis and maize yields for two semi-arid locations in east Africa.** Agricultural and Forest Meteorology, 2003. 117, 23-27.

BETTS, R.; SANDERSON, M.; WOODWARD, S. **Effects of large-scale Amazon forest degradation on climate and air quality through fluxes of carbon dioxide, water, energy, mineral dust and isoprene.** Philosophical Transactions of the Royal Society B: Biological Sciences, 2008. 363, 1873-1880.

BONETT, D. G.; WRIGHT, T. A. **Sample size requirements for Pearson, Kendall, and Spearman correlations.** Psychometrika, 2000. 65, 23-28. https://doi.org/10.1007/bf02294183.

BRASIL, 2012. **Lei nº 12.651 de 25 de maio de 2012**. Casa Civil, Subchefia para assuntos jurídicos. Available in: http://presrepublica.jusbrasil.com.br/legislacao/1032082/lei-12651-12/. (Accessed on May 27, 2018).

BUTT, N.; DE OLIVEIRA P. A.; COSTA M. H. **Evidence that deforestation affects the onset of the rainy season in Rondônia, Brazil.** Journal of Geophysical Research Atmospheres, 2011. 116, D11120. https://doi.org/10.1029/2010JD015174.

BRUIJNZEEL, L. A**. Hydrological functions of tropical forests: Not seeing the soil for the trees?**. Agriculture, Ecosystems and Environment, 2004. 104, 185–228. https://doi.org/10.1016/j.agee.2004.01.015.

CARVALHO, D. F.; FARIA, R. A.; SOUSA, S. A. V; BORGES, H. Q. **Espacialização do período de veranico para diferentes níveis de perda de produção na cultura do milho, na bacia do Rio Verde Grande, MG.** Revista Brasileira de Engenharia Agrícola e Ambiental, 2000. 4, 172-176.

CARVALHO, G.; BARROS, A. C.; MOUTINHO, P.; NEPSTAD, D. **Sensitive Development Could Protect Amazonia Instead of Destroying It.** Nature, 2001. 409, 131.

CEBALLOS, A.; MERTÍNEZ-FERNÁNDEZ, J; LUEGO-UGIDOS, M. A. **Analysis of rainfall trends and dry periods on a pluviometric gradient representative of Mediterranean climate in the Duero Basin, Spain.** Journal of Arid Environments, 2004. 58, 215–233.

CHAMBERS, J. Q.; ARTAXO, P. **Deforestation size influences rainfall.** Nature Climate Change, 2017. 7, 175–176.

COSTA M. H.; FOLEY J. A. **Combined effects of deforestation and doubled atmospheric CO_2 concentrations on the climate of Amazonia.** Journal of Climate, 2000. 13, 18-34.

COSTA, M. H. **Large-scale hydrologic impacts of tropical forest conversion.** In: Bonell, M., Bruijnzeel, L.A. (Eds.), Forests–Water–People in the Humid Tropics. Cambridge University Press, Cambridge, 2004.

COSTA, M. H., BIAJOLI, M. C., SANCHES, L., MALHADO, A. C. M., HUTYRA, L. R., DA ROCHA, H. R., AGUIAR, R. G., DE ARAÚJO, A. C. **Atmospheric versus vegetation controls of Amazonian tropical rain forest evapotranspiration: Are the wet and seasonally dry rain forests any different?**. Journal of Geophysical Research, 2010. 115, G04021. https://doi:10.1029/2009JG001179.

COSTA, M. H.; FOLEY, J. A. **Water balance of the Amazon Basin: Dependence on vegetation cover and canopy conductance.** Journal of Geophysical Research, 1997. 102, 23973-23989.

COSTA, M. H.; PIRES, G. **Effects of Amazon and Central Brazil deforestation scenarios on the duration of the dry season in the arc of deforestation.** International Journal of Climatology, 2010. 30, 1970–1979.

CULF, A. D.; ESTEVES, J. L.; MARQUES FILHO, A. DE O.; DA ROCHA, H. R. **Radiation, temperature and humidity over forest and pasture in Amazonia.** Amazonian Deforestation and Climate, 1996. 175–191.

DAVIDSON, E.; DE ARAÚJO, A.; ARTAXO, P.; BALCH, J.; BROWN, F.; BUSTAMANTE, M.; COE, M.; DEFRIES, R.; KELLER, M.; LONGO, M.; MUNGER, J.; SCHROEDER, W.; FILHO, B.; SOUZA, C.; WOFSY, S. **The Amazon basin in transition.** Nature, 2012. 481, 321–328.

DEBORTOLI, N. S.; DUBREUIL V.; HIROTA M.; RODRIGUES FILHO S.; LINDOSOA D. P.; NABUCETB, J. **Detecting deforestation impacts in Southern Amazonia rainfall using rain gauges.** International Journal of Climatology, 2016. 37, 2889–2900. https://doi.org/10.1002/joc.4886.

DEBORTOLI, N. S.; DUBREUIL, V.; FUNATSU, B.; DELAHAYE F.; DE OLIVEIRA, C. H.; RODRIGUES-FILHO, S.; SAITO, C. H.; FETTER, R.

Rainfall patterns in the Southern Amazon: a chronological perspective (1971–2010). Climate Change, 2015. 132, 251–264, https://doi.org/10.1007/s10584-015-1415-1.

DIAS, L. C. P.; PIMENTA, F. M.; SANTOS, A. B.; COSTA, M. H.; LADLE, R. J. **Patterns of land use, extensification and intensification of Brazilian agriculture.** Global Change Biology, 2016. 22, 2887–2903. https://doi.org/10.1111/gcb.13314.

DOORENBOS, J.; KASSAM, A. H. **Yield response to water.** FAO Irrigation and Drainage Paper, 1979. 33.

DUBREUIL, V.; MEROT, P.; DELAHAYE, D.; DESNOS, P. **Changement climatique dans l'Ouest.** Rennes, Presses Universitaires de Rennes, 2012.

DURIEUX, L. **Etude des relations entre les caractéristiques géographiques de la surface et les nuages convectifs dans la région de l'arc de déforestation en Amazonie.** Thèse de Doctorat de l'Université d'Aix-Marseille I., 2002. 279p.

ERFANIAN A.; WANG G.; FOMENKO L. **Unprecedented drought over tropical South America in 2016: significantly under-predicted by tropical SST.** Scientific Reports, 2017. 7, 5811. https://doi.org/10.1038/s41598-017-05373-2

ESPINOZA, J., RONCHAIL, J., MARENGO, J., SEGURA, H. **Contrasting North–South changes in Amazon wet-day and dry-day frequency and related atmospheric features (1981–2017).** Climate Dynamics, 2018. http://10.1007/s00382-018-4462-2.

ESPINOZA, W.; AZEVEDO, J.; ROCHA, L.D. **Densidade de plantio e irrigação suplementar na resposta de três variedades de milho ao déficit hídrico na região de cerrados.** Pesquisa Agropecuária Brasileira, 1980. 15, 85–95.

ESPINOZA, W.; AZEVEDO, L. G. DE; JARRETA JÚNIOR, M. **O clima da região dos Cerrados em relação à agricultura. Planaltina, DF.** EMBRAPACPAC, 37. (EMBRAPA-CPAC. Circular técnica, 9.

ESPINOZA-VILLAR, J. **Impact de la variabilit climatique sur l'hydrologie du basin amazonien.** Thèse de Doctorat. Université Paris 6, Écoledoctorale "Sciences de L'Environnement d'Ile –de-France". Paris-France, 2009.

FEARNSIDE, P.M. **Deforestation in Brazilian Amazonia: History, rates and consequences.** Conservation Biology, 2005. 3, 680-688.

FERREIRA, V. L.; VENTICINQUE, E.; ALMEIDA, S. **O desmatamento na Amazônia e a importância das áreas protegidas.** Estudos Avançados, 2005. 19, 53.

FETTER R., DE OLIVEIRA C. H., STEINKE E. T. **Um Índice para Avaliação da Variabilidade Espaço-Temporal das Chuvas no Brasil.** Revista Brasileira de Meteorologia, 2018. 33, 2, 225-237. http://dx.doi.org/10.1590/0102-7786332002.

FIGUEROA, S. N.; NOBRE, C. A. **Precipitation distribution over central and western tropical South America.** Climanálise, 1990. 5, 36-45.

FOX P.; ROCKSTRÖM J. **Supplemental irrigation for dry-spell mitigation of rainfed agriculture in the Sahel.** Agricultural Water Management, 2003. 61, 29–50.

FU, R.; LI, W. **The influence of the land surface on the transition from dry to wet season in Amazonia.** Theoretical and Applied Climatology, 2004. 78, 97-110.

FU, R.; YINA L.; WENHONG, L.; ARIASC, P. A.; DICKINSON, R. E.; HUANGA, L.; CHAKRABORTYA, S.; FERNANDES, K.; LIEBMANN, B.; FISHER, R.; RANGA, B. M. **Increased dry-season length over southern Amazonia in recent decades and its implication for future climate projection.** Proceedings of the National Academy of Sciences, 2013. 110, 18110-18115. http://10.1073/ pnas.1302584110.

FU, R; ZHU, B; DICKINSON, E. **How do atmosphere and land surface influence seasonal changes of convection in the tropical amazon?.** Journal of Climate, 1999. 12, 1306.

GAN M. A; KOUSKY V. E; ROPELEWSKI C. F. **The South American monsoon circulation and its relationship to rainfall over west-central Brazil.** Journal of Climate, 2004. 17, 47–66. http://doi.org/10.1175/1520-0442(2004)017<0047:TSAMCA>2.0. CO;2.

GASH, J. H. C.; NOBRE C. A. **Climatic effects of Amazonian deforestation: Some results from ABRACOS.** Bulletin of the American Meteorological Society, 1997. 78, 823– 830, http://doi.org/10.1175/15200477(1997)078<0823:CEOADS>2.0. CO;2.

HANSEN, M. C.; POTAPOV, P.V.; MOORE, R.; HANCHER, M.; TURUBANOVA, S. A.; TYUKAVINA, A.; THAU, D.; STEHMAN, S. V.; GOETZ, S. J.; LOVELAND, T. R.; KOMMAREDDY, A.; EGOROV, A.; CHINI, L. P.; JUSTICE, C. O.; TOWNSHEND, J. R. G. **High-Resolution Global Maps of 21st-Century Forest Cover Change.** Science, 2013. 342, 850-853.

HASTENRATH S. **Annual cycle of upper-air circulation and convective activity over the tropical Americas.** Journal of Geophysical Research Atmospheres, 1997. 102, 4267-4274.

HERNANDEZ, F. B. T.; SOUZA, S. A. V. DE; ZOCOLER, J. L.; FRIZZONE, J. A. **Simulação e efeito de veranicos em culturas desenvolvidas na região de**

Palmeira d'Oeste, Estado de São Paulo. Engenharia Agrícola, 2003. 23, 21-30.

HOREL, J.D.; HAHMANN, A.N.; GCISLER, J.E. **An investigation of the annual cycle of convective activity over the tropical Americas.** Journal of Climate, 1989. 2, 1388-1403. http://10.1590/S0001-37652008000100006.

INSTITUTO NACIONAL DE PESQUISAS ESPACIAIS (INPE). **Monitoramento da Floresta Amazônica Brasileira por Satélite**. Retrieved from http://www.obt.inpe.br/prodes, 2012.

INSTITUTO NACIONAL DE PESQUISAS ESPACIAIS (INPE). **Projeto PRODES: Monitoramento da Floresta Amazônica Brasileira por Satélite**. São José dos Campos, Brazil: INPE. Retrieved from http://www.obt.inpe.br/prodes/, 2017.

KAIMOWITZ, D.; MERTENS, B.; WUNDER, S.; PACHECO, P. **Hamburger Connection Fuels Amazon Destruction.** Bangor, Indonesia, Center for International Forest Research, 2004.

KALNAY E. , M. KANAMITSU, R. KISTLER, W. COLLINS, D. DEAVEN, L. GANDIN, M. IREDELL, S. SAHA, G. WHITE, J. WOOLLEN, Y. ZHU, M. CHELLIAH, W. EBISUZAKI, W. HIGGINS, J. JANOWIAK, K. C. MO, C. ROPELEWSKI, J. WANG, A. LEETMAA, R. REYNOLDS, ROY JENNE*;* DENNIS JOSEPH. **The NCEP/NCAR 40-Year Reanalysis Project.** Bulletin of the American Meteorological Society, 1996. 77, 437-471. http://dx.doi.org/10.1175/1520-0477(1996)077<0437:TNYRP >2.0.CO;2

KHANNA, J.; MEDVIGY, D. **Strong control of surface roughness variations on the simulated dry season regional atmospheric response to contemporary deforestation in Rondônia, Brazil**. Journal of Geophysical Research Atmospheres, 2014. 119, 13067–13078. https://doi.org/10.1002/2014JD022278.

KHANNA, J.; MEDVIGY, D.; FUEGLISTALER, S; WALKO, R. **Regional dry-season climate changes due to three decades of Amazonian deforestation.** Nature Climate Change, 2017. **7**, 200–204 https://doi.org/10.1038/NCLIMATE3226.

LAMBIN E. F.; MEYFROIDT P. **Global land use change, economic globalization, and the looming land scarcity.** Proc. Natl. Acad. Sci., 2011. 108 3465–72

LAURANCE, W.F.; COCHRANE, M.A.; BERGEN, S.; FEARNSIDE, P.M.; DELAMÔNICA, P.; BARBER, C.; D'ANGELO, S.; FERNANDES, T. **The future of Brazilian Amazon.** Science, 2001. 291, 438-439.

LAWRENCE, D.; K. VANDECAR. **Effects of tropical deforestation on climate and agriculture.** Nature Climate Change, 2014. 5, 27-36

LEAN, J.; BUTTON, C. B.; NOBRE, C. A.; ROWNTREE, P. R. **The simulated impact of Amazonian deforestation on climate using measured ABRAÇOS vegetation characteristics.** In: Gash, J.H.C.; Nobre, C.A.; Roberts, J.M.; Victoria, R.L. (eds). Amazonian deforestation and climate. John Wiley, Sons, Chichester. United Kingdom, 1996. 549-576.

LEITE, C. C.; M. H. COSTA; C. A. DE LIMA; C. A. A. S. RIBEIRO; G. C. SEDIYAMA. **Historical reconstruction of land use in the Brazilian Amazon (1940–1995).** Journal of Land Use Science, 2011. 6, 33–52. http://doi.org/10.1080/ 1747423X.2010.501157.

LEITE-FILHO, A. T., SOUSA PONTES, V. Y., AND COSTA, M. H. Effects **of deforestation on the onset of the rainy season and the duration of dry spells in southern Amazonia.** Journal of Geophysical Research: Atmospheres, 2019. 124. https://doi.org/10.1029/2018JD029537

LI, W.; FU, R. **Influence of Cold Air Intrusions on the Wet Season Onset over Amazonia**. Journal of Climate, 2006. 19, 257–275.

LIEBMANN, B.; CAMARGO, S.J.; SETH, A.; MARENGO, J.A.; CARVALHO, L.M.V.; ALLURED, D.; FU, R; VERA, C.S. **Onset and end of the rainy season in South America in observations and the ECHAM 4.5 atmospheric general circulation model.** Journal of Climate, 2007. 20, 2037-2050. http://doi.org/10.1175/JCLI4122.

LIEBMANN, B.; MECHOSO, C. R. **The South American Monsoon System.** In: The Global Monsoon System: Research and Forecast (2nd Edition), 2011. edited by Chih-Pei Chang. 137-157.

MACEDO N. M.; DEFRIES, R.S.; MORTON, D. C.; STICKLER, C. M.; GALFORD, G. L.; SHIMABUKURO, Y. E.. **Decoupling of deforestation and soy production in the southern Amazon during the late 2000s.** PNAS, 2012. 109, 1341-1346. https://doi.org/10.1073/pnas.1111374109.

MAIA ALVES, S. F., G. FISCH; I. F. VENDRAME. **Modificações do microclima e regime hidrológico devido ao desmatamento na Amazônia.** Acta Amazon, 1999. 29, 395–409.

MAKARIEVA, A.; GORSHKOV, V.; LI, B. L. **Revisiting forest impact on atmospheric water vapor transport and precipitation.** Theoretical and Applied Climatology, 2012. 111, 79-96. http://dx.doi.org/10.1007/s00704-012-0643-9.

MALHI, Y.; ROBERTS, J.T.; BETTS, R.A.; KILLEEN, T.J.; LI, W.; NOBRE, C.A. **Climate Change, Deforestation, and the Fate of the Amazon.** Science, 2008. 319, 169-172.

MALHI, Y.; ROBERTS, J.T.; BETTS, R.A.; KILLEEN, T.J.; LI, W.; NOBRE, C.A. **Climate Change, Deforestation, and the Fate of the Amazon.** Science, 2008. 319, 169-172.

MARENGO J. **Interdecadal variability and trends of rainfall across the Amazon Basin.** Theoretical and Applied Climatology, 2004. 78, 79-96. http://doi.org/10.1007/s00704-004-0045-8.

MARENGO, J. A.; LIEBMANN, B.; KOUSKY, V. E.; FILIZOLA, N. P.; WAINER, I. C. **Onset and end of the rainy season in the Brazilian Amazon Basin.** Journal of Climate, 2001. 14, 833– 852.

MARENGO J., SOARES W., SAULO C., NICOLINI M., 2004. Climatology of the LLJ east of the Andes as derived from the NCEP.

MARENGO, J. A.; NOBRE, C.A.; CHOU, S. C.; TOMASELLA, J.; SAMPAIO, G.; ALVES, L. M.; OBREGÓN, G. O.; SOARES, W. R.; BETTS, R.; KAY, G. **Riscos das mudanças climáticas no Brasil: análise conjunta Brasil-Reino Unido sobre os impactos das mudanças climáticas e do desmatamento na Amazônia.** http://www.ccst.inpe.br/wp-content/uploads, 2011.

MARENGO, J. **Interannual variability of deep convection in the tropical South American sector as deduced from ISCCP C2 data.** International Journal of Climatology, 1995. 15, 995-1010.

MARENGO, J. **Interannual variability of surface climate in the Amazon basin.** International Journal of Climatology, 1992. 12, 853-863.

MARENGO, J. **Interdecadal variability and trends of rainfall across the Amazon basin.** Theoretical and Applied Climatology, 2004. 78, 79-96.

MARENGO, J. **Variations and Change in South American Streamflow.** Climate Change, 1995. 31, 99-117.

MARENGO, J.A. **On the Hydrological Cycle of the Amazon Basin: a historical review and current state-of-the-art.** Revista Brasileira de Meteorologia, 2006. 21, 1-19.

MCHUGH, O. V.; STEENHUIS, T. S.; ABEBE, B; FERNANDES, E. C. M. **Performance of in situ rainwater conservation tillage techniques on dry spell mitigation and erosion control in the drought-prone North Wello zone of the Ethiopian highlands.** Soil & Tillage Research, 2007. 97, 19-36.

MINUZZI, R. B.; SEDIYAMA, G. C.; RIBEIRO, A.; COSTA, J. M. N. **"El Niño: ocorrência e duração dos veranicos do Estado de Minas Gerais".** Revista Brasileira de Engenharia Agrícola e Ambiental, 2005. 9, 364-371.

MORTON D. C., DEFRIES S. R., SHIMABUKURO E. Y., ANDERSON L., ARAI E., ESPIRITO-SANTO F. DEL B., FREITAS R.; MORISETTE J. **Cropland expansion changes deforestation dynamics in the southern Brazilian Amazon.** Proceedings of the National Academy of Sciences, 2006. 103, 14637-14641.

NEPSTAD, D.; CARVALHO, G.; BARROS, A. C.; ALENCAR, A; CAPOBIANCO, J. B.; BISHOP, J; MOUTINHO, P.; LEFEBVRE, P. E;

SILVA, U. L. **Road paving, fire regime feedbacks, and the future of Amazon forests.** Forest Ecology and Management, 2001. 154, 395- 407.

NOBRE C. A.; SAMPAIO G.; BORMA L. S.; CASTILLA-RUBIO J. C.; SILVA J. S.; CARDOSO M. **Land-use and climate change risks in the Amazon and the need of a novel sustainable development paradigm.** Proceedings of the National Academy of Sciences, 2006. 113, 10759-10768.

NOBRE, P.; M. MALAGUTTI; D. F. URBANO; R. A. F. DE AMEIDA; E. GIAROLLA. **Amazon deforestation and climate change in a coupled model simulation.** Journal of Climate, 2009. 22, 5686-5697. http://doi.org/10.1175/2009JCLI2757.1.

ODEKUNLE, T. O.; BUYIRO, S. O. G. **Rain days predictability in southwestern Nigeria.** Journal of Nigerian Meteorological Society, 2003. 4, 1-17.

OECD-FAO. **OECD-FAO Agricultural Outlook 2015–2024**, 2015. 10.1787/agr outlook-2015-en.

OLIVEIRA, A. D. **Aspectos agroclimáticos do arroz de sequeiro no estado de Minas Gerais.** UFV, Viçosa, MG, 2000. 56p.

OLIVEIRA, G. S.; SATYAMURTY, P. **"O El Niño de 1997/98: Evolução e impactos no Brasil,"1998.** in SBMET, Anais do X Congresso Brasileiro de Meteorologia, CD-ROM. Available online at: http://www.cbmet.com/edicoes. php?pageNum_Recordset_busca=8&totalRows_Recordset_busca=623&cgid= 13&imageField2.x=51&imageField2.y=11

PANDAY P. K.; COE M. T.; MACEDO M. N.; LEFEBVRE P.; CASTANHO A. D. DE A. **Deforestation demises water balance changes due to climate variability in the Xingu River in eastern Amazonia**. Journal of Hydrology, 2015. 523 822–829.

PEBESMA E; HEUVELINK G. **Spatio-temporal interpolation using gstat.** RFID Journal, 2016. 8, 204–218.

PEBESMA, E. J. **Multivariable geostatistics in S: the gstat package.** Computers & Geosciences, 2004. 30, 683-691.

POHLKER C.; WIEDEMANN K. T.; SINHA B. **Biogenic potassium salt particles as seeds for secondary organic aerosol in the Amazon.** Science, 2012. 337, 1075-1078.

RAMOS DA SILVA, R; GANDU A. W.; SÁ, L. D. A; SILVA DIAS, M. A. F. **Cloud streets and land water interactions in the Amazon.** Biogeochemistry (Dordrecht), 2011. 105, 201-211.

RAY, D. R. K.; JONATHAN A FOLEY. **Increasing global crop harvest frequency: recent trends and future directions.** Environmental Research Letter, 2013. 8, 044041. doi:10.1088/1748-9326/8/4/044041

RIZZO L.V.; ARTAXO P.; MÜLLER T.; WIEDENSOHLER A.; PAIXÃO M.; CIRINO G.G.; ARANA A.; SWIETLICKI E.; ROLDIN P.; FORS E.O.; WIEDEMANN K.T.; LEAL L.S.M.; KULMALA M. **Long term measurements of aerosol optical properties at a pristine forest site in Amazonia.** Atmospheric Chemistry and Physics, 2012. 12, 23333-23401.

RONCHAIL, J.; COCHONNEAU, G.; MOLINIER, M.; GUYOT, J.L.; CHAVES, A.G.D.; GUIMARAES, V.; DE OLIVEIRA, E. **Interannual rainfall variability in the Amazon basin and sea-surface temperatures in the equatorial Pacific and the tropical Atlantic Oceans.** International Journal of Climatology, 2002. 22, 1663-1686.

SALATI, E., A; DALL'OLIO, E; MATSUI; J. R. GAT. **Recycling of Water in the Amazon, Brazil: an isotopic study.** Water Resources Research, 1979. 15, 1250-1258.

SALAZAR, L. F.; NOBRE, C. A.; OYAMA, M. D. **Climate change consequences on the biome distribution in tropical South America.** Geophysical Research Letters, 2007. 34. http:10.1029/2007GL029695.

SAMPAIO, G.; NOBRE C.; COSTA, M.H.; SATYAMURTY, P.; SOARES-FILHO, B. S.; CARDOSO, M. **Regional climate change over eastern Amazonia caused by pasture and soybean cropland expansion**. Geophysical Research Letters, 2007. 34, L17709, http://dx.doi.org/10.1029/2007GL030612.

SATYAMURTY, P.; da COSTA, C.P.W.; MANZI, A.O. **Moisture source for the Amazon Basin: a study of contrasting years.** Theoretical and Applied Climatology, 2013. 111, 195-209.

SATYAMURTY, P.; da COSTA, C.P.W.; MANZI, A.O. **Moisture source for the Amazon Basin: a study of contrasting years.** Theoretical and Applied Climatology, 2013. 111, 195-209.

SCHUBERT, S. D.; SUAREZ, M. J.; PEGION, P. J.; RANDAL D. K.; BACMEISTER J. T. **Causes of long-term drought in the United States Great Plains.** Journal of Climate, 2004. 17, 485- 503.
services. Anais da Academia Brasileira de Ciências, 2008. 80, 101–114.

SHAPIRO, S.S.; WILK, M.B. **An analysis of variance test for normality (complete samples).** Biometrika, 1965. 52, 591–611.

SHARMA, T. C. **Simulation of the Kenyan longest dry and wet spells and the largest rain-sums using a Markov Model.** Journal of Hydrology, 1996. 178, 55-67.

SHEIL, D.; MURDIYARSO, D. **How forests attract rain: an examination of a new hypothesis.** Bioscience, 2009. 4, 341–347.

SILVA, F. A. S.; RAO, T. V. R. **Regimes pluviais, estação chuvosa e probabilidade de ocorrência de veranicos no estado do Ceará.** Revista Brasileira de Engenharia Agrícola e Ambiental, 2002. 6, 453-459.

SLEIMAN, J. **Veranicos ocorridos na porção noroeste do estado do rio Grande do Sul entre 1978 e 2005 e sua associação às condições climáticas na atmosfera.** Dissertação de Mestrado, Universidade de São Paulo, Departamento de Geografia, São Paulo, SP, 2008. 164.

SOARES, D. B.; NÓBREGA, R. S. **Análise espacial e climatológica da ocorrência de veranicos no sertão de Pernambuco.** Revista de Geografia, 2010. 27, 95-106.

SOMBROEK, W. **Spatial and Temporal Patterns of Amazon Rainfall.** AMBIO, 2001. 30, 388396. https://doi.org/10.1579/0044-7447-0.7.388.

SPANGLER, K. R.; LYNCH, A. H.; SPERA, S. A. **Precipitation drivers of cropping frequency in the Brazilian Cerrado: evidence and implications for decision-making.** Weather, Climate, and Society, 2017. 9, 201-213. http://dx.doi.org/10.1175/WCAS-D-16-0024.1.

SPEARMAN, C. E. **The proof and measurement of association between two things.** American Journal of Psychology, 1904. 15, 72–101.

STERN, R. D.; COE, R. **The use of rainfall models in agricultural planning.** Agricultural Meteorology, 1982. 26, 35-50.

STRAND, J.; SOARES-FILHO, B.; COSTA, M. H.; OLIVEIRA, U.; RIBEIRO, S. C.; PIRES, G. F.; OLIVEIRA, A; RAJÃO, R.; MAY, P.; VAN DER HOFF, R.; SIIKAMÄKI, J.; MOTTA, R. S.; TOMAN, M. **Spatially explicit valuation of the Brazilian Amazon Forest's Ecosystem Services.** Nature Sustainability. 1, 657-664.

SUGAHARA, S. **Flutuações interanuais, sazonais e inatrasazonais da precipitação no estado de São Paulo.** Ph.D. thesis, Universidade de São Paulo, 1991. 140.

SUMILA, T.C.A; PIRES, G.F.; FONTES, V. F.; COSTA, M. H. **Sources of water vapor to economically relevant regions in Amazonia and the effect of deforestation.** Journal of Hydrometeorology, 2017. 18, 1643-1655. http://dx.doi.org/10.1175/JHM-D-16-0133.1

VERBURG R.; RODRIGUES FILHO S.; DEBORTOLI N.; LINDOSO D. P.; NESHEIM I.; BURSZTYN M. **Evaluating sustainability options in an agricultural frontier of the Amazon using multi-criteria analysis.** Land Use Policy, 2014b. 37, 27–39.

VERBURG, R.; RODRIGUES FILHO, S.; LINDOSO, D. P.; DEBORTOLI, N.; LITRE, G; BURSZTYN, M. **The impact of commodity price and conservation policy scenarios on deforestation and agricultural land use in a frontier area within the Amazon.** Land Use Policy, 2014a. 37, 14-26.

VILLAR, J. C. E.; RONCHAIL, J.; GUYOT, J. L.; COHONNEAU, G.; NAZIANO, F.; AVADO, W.; OLIVEIRA, E.; POMBOSAG, R; VAUCHELH, P. **Spatiotemporal rainfall variability in the Amazon basin countries (Brazil, Peru, Bolivia, Colombia, and Ecuador).** International Journal of Climatology, 2009. 29, 1574-1594. https://doi.org/10.1002/joc.179.

WAHA, K; VAN BUSSEL, L; MÜLLER, C; BONDEAU, A. **Climate driven simulation of global crop sowing dates.** Global Ecology and Biogeography, 2012. 21, 247-259.

WRIGHT, I. R.; J. H. C. GASH; H. R. DA ROCHA; W. J. SHUTTLEWORTH; C. A. NOBRE; G. T. MAITELLI; C. A. G. P. ZAMPARONI; P. R. A. CARVALHO. **Dry season micrometeorology of central Amazonian.** Meteoroly Society, 1992. 118, 1083–1099.

WRIGHT, J.; FU, R.; JOHN, W. R.; CHAKRABORTY, S.; E. CLINTON, N. E.; RISI, C.; SUN, Y.; YIN, L. **Rainforest-initiated wet season onset over the southern Amazon.** Proceedings of the National Academy of Sciences, 2017. 114, 8481-8486. https://doi.org/10.1073/pnas.1621516114.

YIN, L.; FU, R.; ZHANG, Y.F.; ARIAS, P.A.; FERNANDO, D.N.; LI, W.; FERNANDES, K.; BOWERMAN, A.R. **What controls the interannual variation of the wet season onsets over the Amazon?**. Journal of Geophysical Research Atmospheres, 2014. 119, 2314–2328. http://doi:10.1002/2013JD021349.

Appendix A

Table A1 - Meteorological stations and data series information

Station	ANA Code	Name	State	Latitude (deg)	Longitude (deg)	Times series	Duration (years)
01	0655001	Km 1027 da BR-163	PA	-7,51083	-55,2636	1983-2012	27
02	0662001	Juma	AM	-7,00833	-62,7872	1993-2012	17
03	0755000	Novo Progresso	PA	-7,06056	-55,4078	1998-2012	13
04	0759000	Vila do Apui	AM	-7,20444	-59,8931	1983-2012	30
05	0760000	Prainha Velha	AM	-7,205	-60,6436	1975-2012	36
06	0760001	Boca do Guariba	AM	-7,70528	-60,5783	1978-2012	35
07	761002	Fazenda Água Azul	AM	-7,82278	-61,2442	1991-2012	22
08	0761003	Fazenda Bela Vista	AM	-7,85333	-61,3339	2004-2011	8
09	0762002	Maici-mirim	AM	-7,63083	-62,6606	1994-2012	19
10	0762003	Maici-grande	AM	-7,80278	-62,3478	1999-2012	14
11	0763001	Humaitá	AM	-7,51528	-63,0286	1983-2009	19
12	0764003	Cristo	AM	-7,465	-64,2433	1976-2012	25
13	0765000	Cachoeira	AM	-7,71556	-66,0583	1978-2012	31

Table A1 - Continuation – Meteorological stations and data series information

14	0765001	São Bento	AM	-7,53056	-65,35	1983-2012	23
15	0851000	Fazenda Rio Dourado	PA	-8,34639	-51,4428	2000-2012	10
16	0855000	KM 947 BR-163	PA	-8,18722	-55,1194	1978-2012	32
17	0857000	Santa Rosa	MT	-8,87028	-57,4164	1983-2012	25
18	0861001	Bodocó	AM	-8,48333	-61,5333	1998-2004	7
19	0861002	Bonamigo	AM	-8,00167	-61,7497	2005-2011	7
20	0862000	Tabajara	RO	-8,93222	-62,0556	1978-2012	31
21	0863005	Sítio Vista Alegre	AM	-8,09778	-63,6475	1983-2010	21
22	0863008	Porto Velho	RO	-8,74194	-63,9025	2002-2009	8
23	0865000	Fazenda Sheffer	AM	-8,33444	-65,7194	1983-2012	25
24	0954001	Cachimbo	MT	-9,81861	-54,8864	1985-2012	24
25	0954002	Guaranta do Norte	MT	-9,97556	-54,9042	2005-2012	6
26	0956001	Jusante Foz Peixoto de Azevedo	MT	-9,64333	-56,0186	1994-2012	23
27	0956002	Paranaita	MT	-9,69389	-56,4742	2000-2012	13
28	0957001	Novo Planeta	MT	-9,56639	-57,3947	1994-2012	22

Table A1 - Continuation – Meteorological stations and data series information

29	0957002	Nova Monte Verde	MT	-9,97694	-57,4739	2001-2012	11
30	0958002	Colniza	MT	-9,45611	-58,2242	2001-2012	9
31	0958004	Cotriguaçu	MT	-9,91333	-58,5642	2005-2012	8
32	0961003	Fábio (boliche)	RO	-9,68139	-61,9789	1987-2012	23
33	0962000	Mineração Oriente Novo	RO	-9,58639	-62,3939	1979-2012	28
34	0962001	Mineração Jacundá	RO	-9,17917	-62,9531	1981-2006	23
35	0963001	Santo Antônio BR-364	RO	-9,26056	-63,1619	1978-2012	32
36	0963004	Fazenda Rio Branco	RO	-9,88722	-62,9878	1981-2011	29
37	0963009	Ponte do Rio Preto do Crespo	RO	-9,46667	-63,25	1998-2011	13
38	0964005	Jaciparaná	RO	-9,25	-64,4	2004-2011	8
39	1052000	Vila São José do Xingu	MT	-10,8072	-52,7461	1977-2012	31
40	1052001	Rio Comandante Fontoura	MT	-10,5547	-52,1833	2000-2012	13
41	1052002	Jusante Rio Preto	MT	-10,0472	-52,1144	2001-2012	11
42	1053001	Fazenda Santa Emília	MT	-10,5392	-53,6089	1977-2012	27
43	1054000	Agropecuária Cajabi	MT	-10,7461	-54,5461	1977-2012	27
44	1054002	Matupá	MT	-10,1503	-54,9189	2005-2012	8

Table A1 - Continuation – Meteorological stations and data series information

45	1055000	Estrada Cuiabá - Santarém	MT	-10,2203	-54,9711	2004-2012	7
46	1055001	Indeco	MT	-10,1125	-55,57	1976-2012	30
47	1055003	Fazenda Tratex	MT	-10,9542	-55,5486	1995-2012	17
48	1055004	Terra Nova do Norte	MT	-10,6044	-55,1033	2001-2011	10
49	1056001	Estância Buriti	MT	-10,3894	-56,4172	2001-2012	10
50	1057001	Trivelato	MT	-9,94167	-57,1331	1983-2012	24
51	1058002	Núcleo Ariel	MT	-9,85639	-58,2489	1983-2012	23
52	1058003	Juruena	MT	-10,3125	-58,5017	1985-2009	22
53	1058004	Novo Tangara	MT	-10,8342	-58,8033	1985-2012	20
54	1058005	Vale do Natal	MT	-10,5886	-58,8678	1986-2012	21
55	1058006	Rio Arinos	MT	-10,6397	-58,0039	2002-2012	10
56	1059000	Humboldt	MT	-10,1753	-59,4517	1979-2012	34
57	1060001	Fazenda Muiraquita	MT	-10,4344	-60,5572	2000-2011	12
58	1061001	Ji-Paraná	RO	-10,8494	-61,9306	1976-1996	20
59	1061002	Fazenda castanhal	MT	-10,3969	-61,0453	1983-2012	20
60	1061003	Rondominas (barrocas)	RO	-10,5169	-62,0014	1987-2011	23

Table A1 - Continuation – Meteorological stations and data series information

61	1062001	Jaru	RO	-10,4458	-62,4656	1977-2011	31
62	1062002	Seringal 70	RO	-10,2364	-62,6272	1979-2012	33
63	1062003	Mirante da serra	RO	-11,0036	-62,6561	1984-2012	24
64	1062004	Theobroma	RO	-10,2364	-62,3458	1987-2012	23
65	1063000	Escola Caramurú	RO	-10,505	-63,6461	1979-2012	28
66	1063002	Buritis	RO	-10,2806	-63,7358	2011	1
67	1152001	Espigão	MT	-11,3933	-52,235	1985-2010	19
68	1154000	Rancho de Deus	MT	-11,0028	-54,8053	1984-2011	22
69	1154001	Santa Felicidade	MT	-11,9292	-54,9981	1983-2012	24
70	1154002	Fazenda Rio Negro	MT	-11,5242	-54,3589	2000-2012	11
71	1154004	Claúdia	MT	-11,4933	-54,8656	2005-2012	7
72	1154005	Riacho de Deus	MT	-11,1272	-54,4767	2007-2012	6
73	1156001	Sinop (Fazenda Sempre Verde)	MT	-11,6914	-55,4486	1984-2012	26
74	1156002	Tabaporã	MT	-11,3047	-56,825	2005-2012	7
75	1156003	Nova Americana	MT	-11,6447	-56,1572	2005-2012	7

Table A1 - Continuation – Meteorological stations and data series information

76	1157000	Porto dos Gaúchos	MT	-11,5358	-57,4172	1974-2010	27
77	1157001	Juara	MT	-11,2531	-57,5067	1984-2012	28
78	1157002	Olho d'água	MT	-11,715	-57,0419	2000-2012	12
79	1158002	Juína	MT	-11,4081	-58,7186	1985-2012	26
80	1158003	Fazenda Tombador	MT	-11,7178	-58,0472	1985-2012	24
81	1158004	Castanheira	MT	-11,14	-58,6161	2005-2012	6
82	1159000	Boteco dos mineiros	MT	-11,845	-59,3394	1985-2011	25
83	1160000	Marco Rondon	RO	-12,0153	-60,855	1978-2012	31
84	1161000	Vista Alegre	RO	-11,4408	-61,4839	1978-2011	31
85	1161001	Pimenta Bueno	RO	-11,6836	-61,1922	1980-2012	31
86	1161002	Rolim de Moura	RO	-11,7497	-61,7764	1984-2012	25
87	1161003	Ministro Andreazza	RO	-11,1969	-61,5281	1987-2002	15
88	1162003	São Miguel do Guaporé	RO	-11,7325	-62,8025	2011-2012	2
89	1163000	São Francisco do Guaporé	RO	-11,9664	-63,2722	2011-2012	2
90	1254001	Agrovensa	MT	-12,8131	-54,7517	1983-2009	17
91	1254002	Consul	MT	-12,3658	-54,4892	1998-2011	11

Table A1 - Continuation – Meteorological stations and data series information

92	1254003	Agropecuária Três Irmãos	MT	-12,7978	-54,2486	2001-2011	10
93	1255001	Teles Pires	MT	-12,675	-55,7931	1977-2012	24
94	1255002	Núcleo Colonial Rio Ferro	MT	-12,5178	-54,9125	1977-2012	26
95	1256002	Fazenda Divisão	MT	-12,9806	-56,3156	2000-2012	11
96	1257000	Brasnorte	MT	-12,1164	-58,0003	1985-2012	26
97	1258001	Fazenda Floresta	MT	-12,8675	-58,0703	2001-2012	7
98	1259001	Cachoeirinha	MT	-12,0603	-59,6503	1985-2005	19
99	1260006	Chupinguaia	RO	-12,5606	-60,9042	2007-2012	5
100	1261001	Parecis	RO	-12,2092	-61,6286	2000-2012	13
101	1262001	Izidolândia	RO	-12,6014	-62,1783	2000-2012	11
102	1354000	Fazenda Agrochapada	MT	-13,4483	-54,2811	1983-2011	27
103	1354001	Agropecuária Malp	MT	-13,3417	-54,0772	2000-2012	11
104	1354002	Fazenda Itaguaçu	MT	-13,1381	-54,4439	2005-2011	7
105	1355001	Porto Roncador	MT	-13,5564	-55,3317	1985-2008	22
106	1356004	São José do Rio Claro	MT	-13,445	-56,7275	2005-2012	7

Table A1 - Continuation – Meteorological stations and data series information

107	1357000	Nova Maringá	MT	-13,0661	-57,1133	1983-2012	25
108	1358002	Fazenda Tucunaré	MT	-13,4667	-58,975	1984-2012	27
109	1358003	Utiariti	MT	-13,0333	-58,2833	1984-1986	3
110	1358007	Aldeia Sacre II	MT	-13,0239	-58,1889	2005-2012	6
111	1359000	Padronal	MT	-13,1831	-59,8769	1984-2012	27
112	1360000	Colorado do Oeste	RO	-13,1142	-60,5483	1984-2011	27